Physics and Applications of Metallic Magnetic Calorimeters

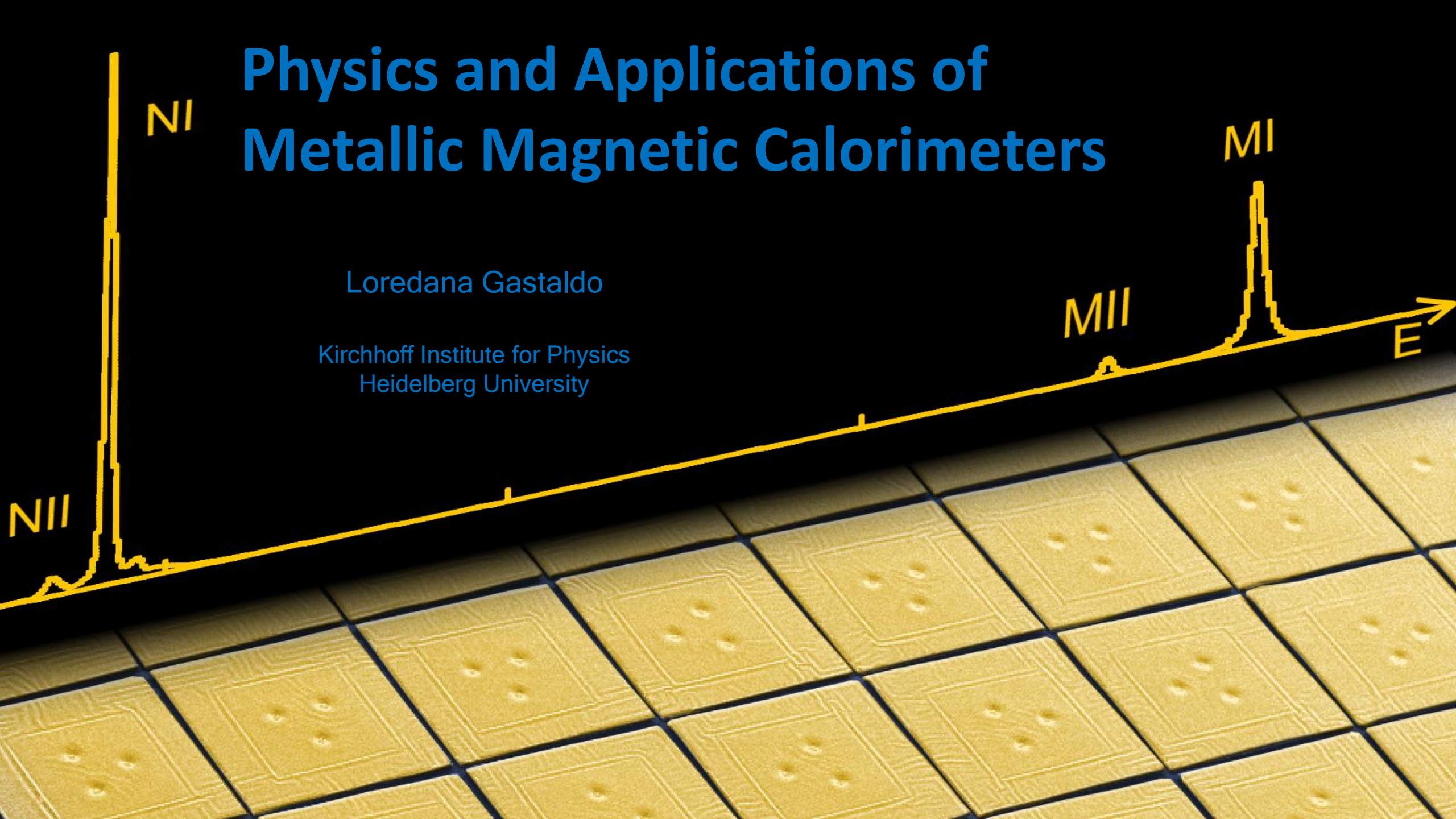

Loredana Gastaldo

Kirchhoff Institute for Physics
Heidelberg University

Outline

- Metallic magnetic calorimeters
  - Thermodynamical properties
  - Readout
- MMC applications and performance
  - x-ray – IAXO
  - Neutrino mass – ECHo
- Conclusions

Low Temperature Calorimeters

Near equilibrium detectors

Energy deposition induces increase of temperature

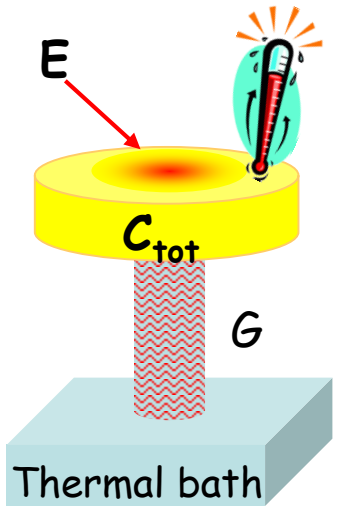

$$\Delta T \cong \frac{E}{C_{tot}}$$

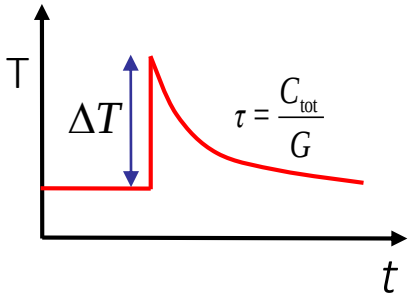

- Very small volume
- Working temperature below 100 mK
  small specific heat
  small thermal noise
- **Very sensitive temperature sensors**

Low Temperature Calorimeters

Near equilibrium detectors

Energy deposition induces increase of temperature

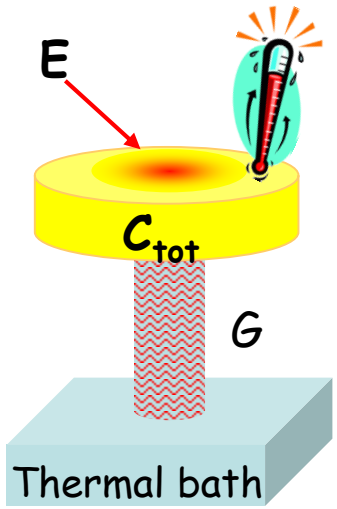

$$\Delta T \cong \frac{E}{C_{tot}}$$

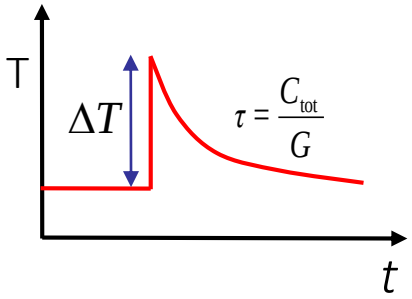

- Very small volume
- Working temperature below 100 mK
  small specific heat
  small thermal noise
- **Very sensitive temperature sensors**

Resistance of highly doped semiconductors

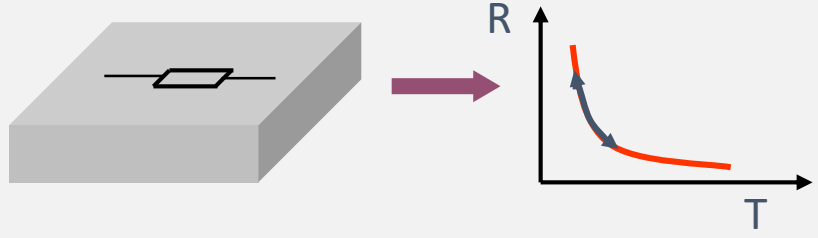

Resistance at superconducting transition,TES

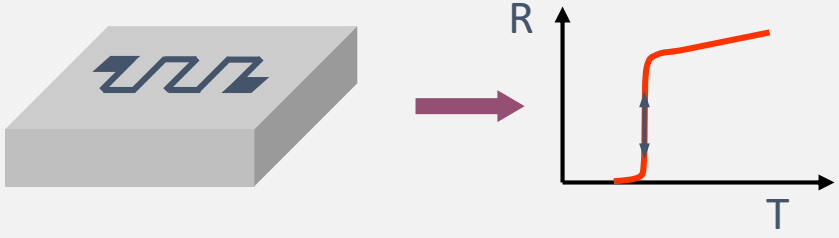

Magnetization of paramagnetic material, MMC

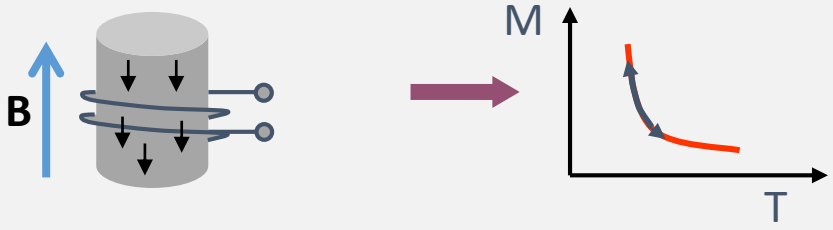

Metallic Magnetic Calorimeters

A.Fleischmann, C. Enss and G. M. Seidel,
Topics in Applied Physics **99** (2005) 63

A.Fleischmann et al.,
AIP Conf. Proc. **1185** (2009) 571

Paramagnetic temperature sensor

Dilute alloy Au:Er or Ag:Er (Er concentration: a few hundred ppm)

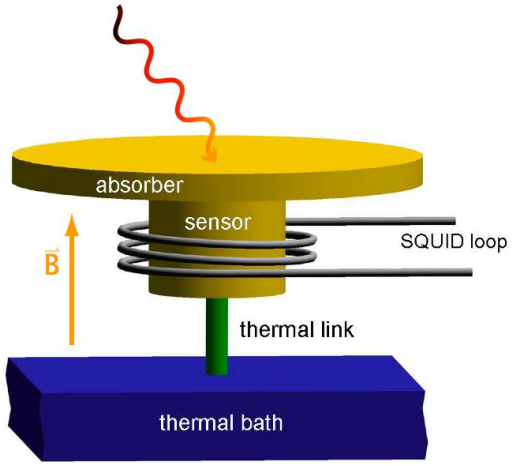

$$\Delta T \cong \frac{E}{C_{\mathrm{tot}}}$$

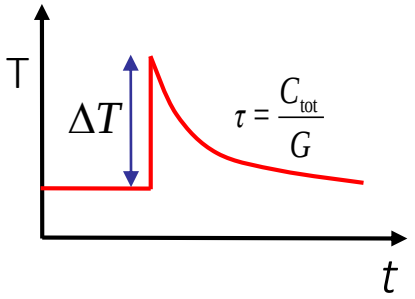

Metallic Magnetic Calorimeters

A.Fleischmann, C. Enss and G. M. Seidel,
Topics in Applied Physics **99** (2005) 63

A.Fleischmann et al.,
AIP Conf. Proc. **1185** (2009) 571

Paramagnetic temperature sensor

Dilute alloy Au:Er or Ag:Er (Er concentration: a few hundred ppm)

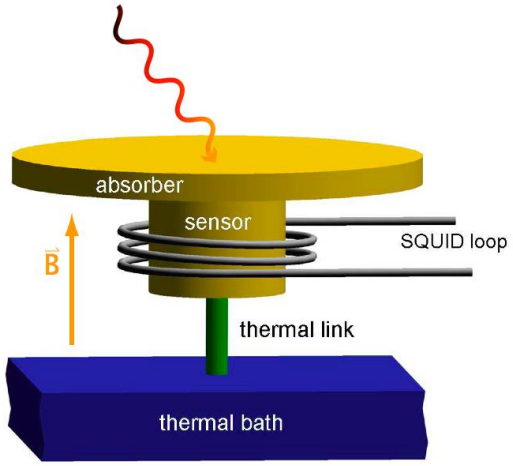

$$\Delta T \cong \frac{E}{C_{tot}} \xrightarrow{\text{MMC}} \Delta\Phi_S \propto \frac{\partial M}{\partial T}\Delta T \rightarrow \Delta\Phi_S \propto \frac{\partial M}{\partial T}\frac{E}{C_{tot}}$$

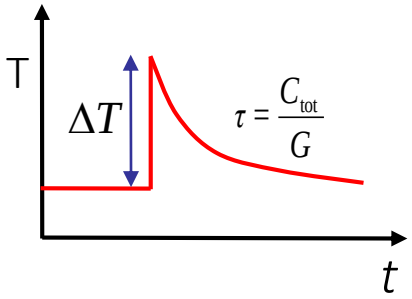

Metallic Magnetic Calorimeters

A.Fleischmann, C. Enss and G. M. Seidel,
Topics in Applied Physics **99** (2005) 63

A.Fleischmann et al.,
AIP Conf. Proc. **1185** (2009) 571

Paramagnetic temperature sensor

Dilute alloy Au:Er or Ag:Er (Er concentration: a few hundred ppm)

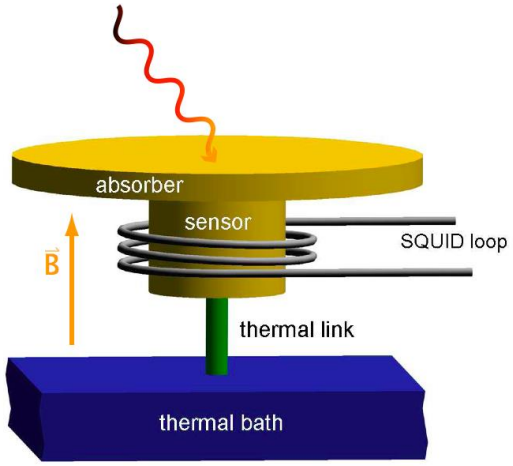

$$\Delta T \cong \frac{E}{C_{tot}} \xrightarrow{\text{MMC}} \Delta\Phi_S \propto \frac{\partial M}{\partial T}\Delta T \rightarrow \Delta\Phi_S \propto \frac{\partial M}{\partial T}\frac{E}{C_{tot}}$$

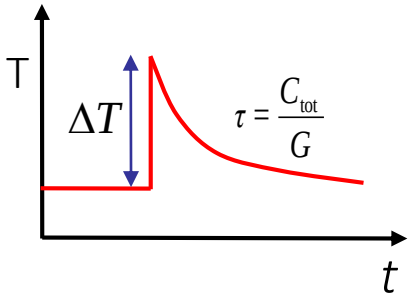

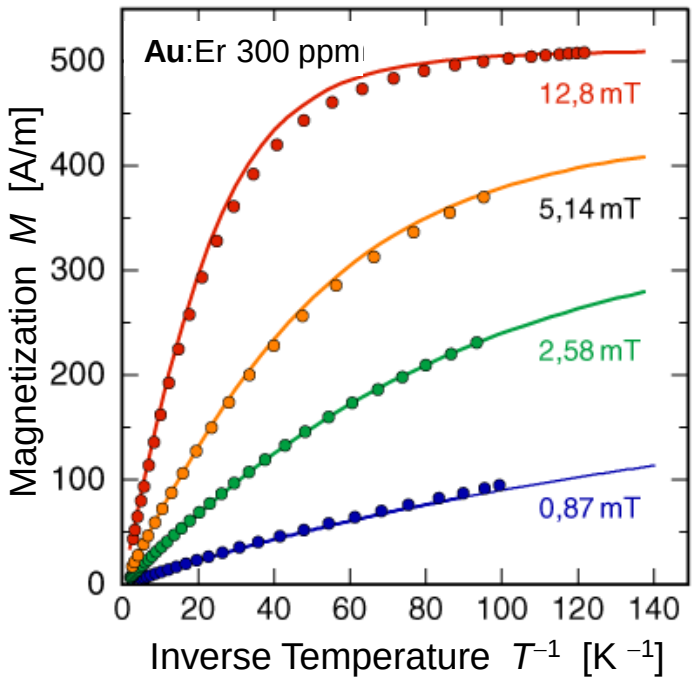

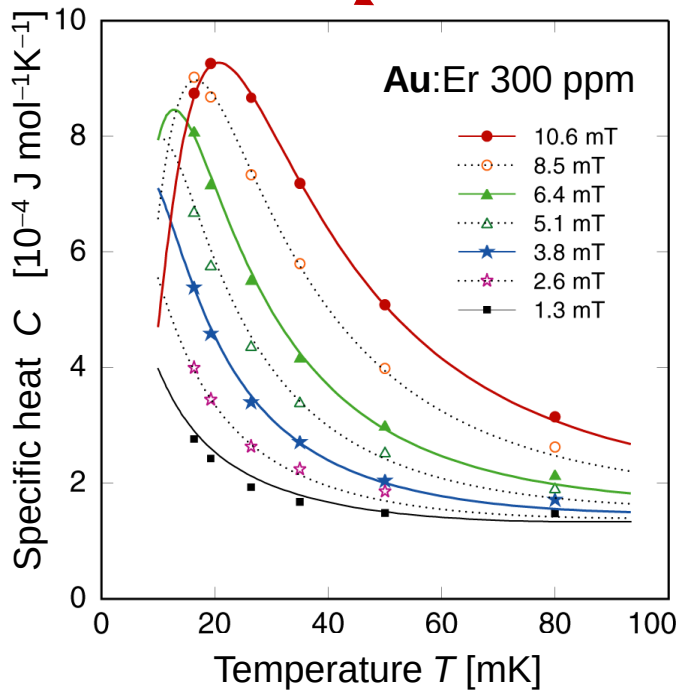

Very good agreement between data and theoretical expectation for interacting spin system

Performance

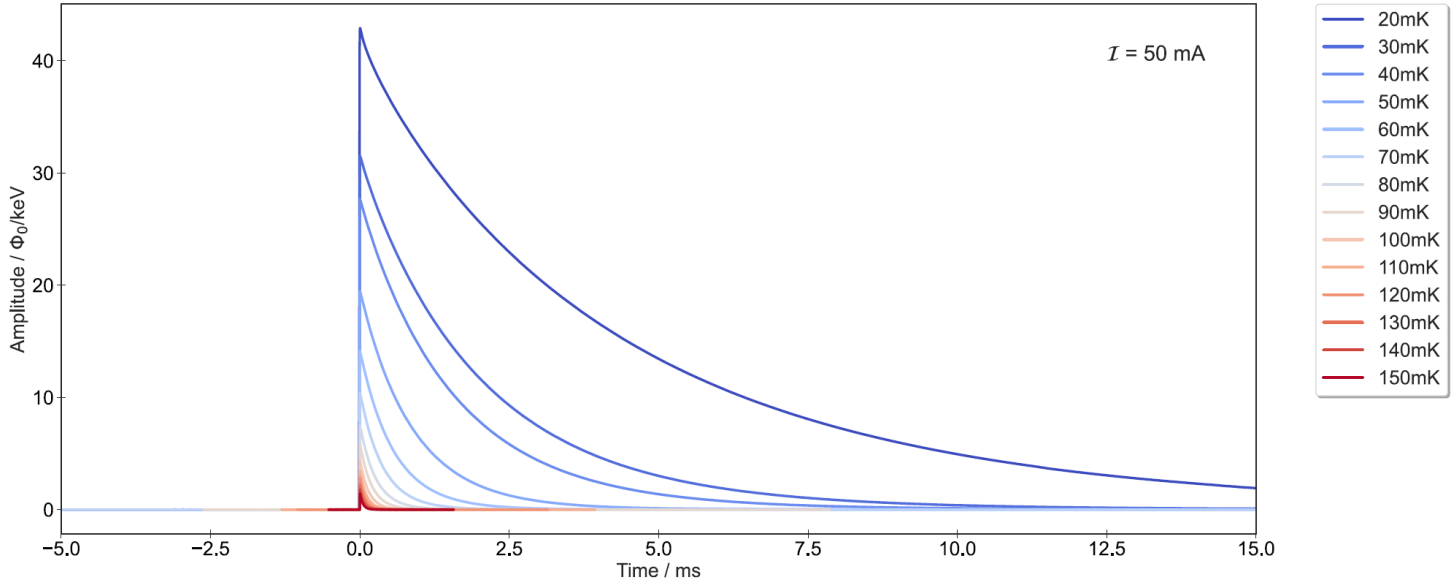

Operation over a large temperature range
→ operation of large arrays

Large dynamic range
→ no saturation of the signal

Design defined decay constant
→ thermal link optimized for detector heat capacity at operating temperature

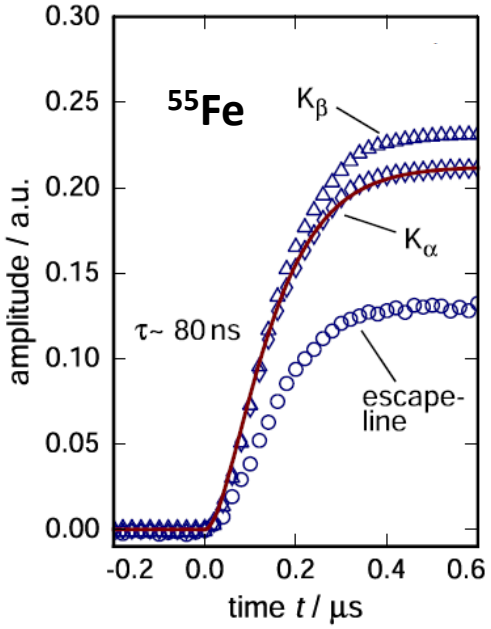

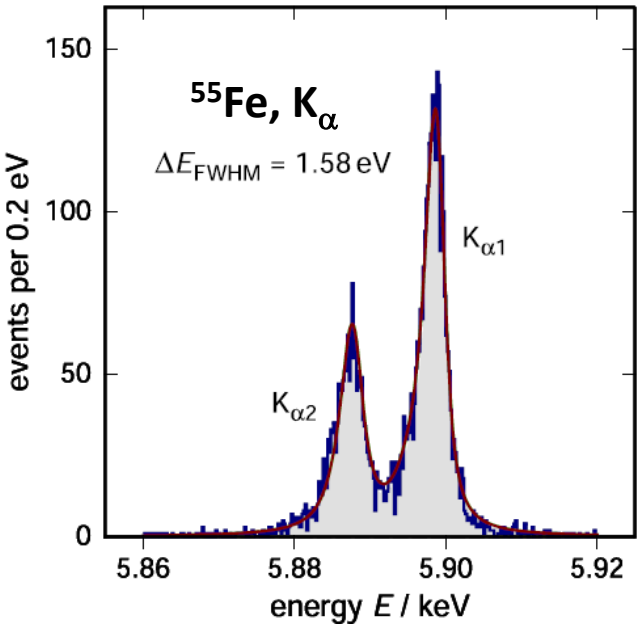

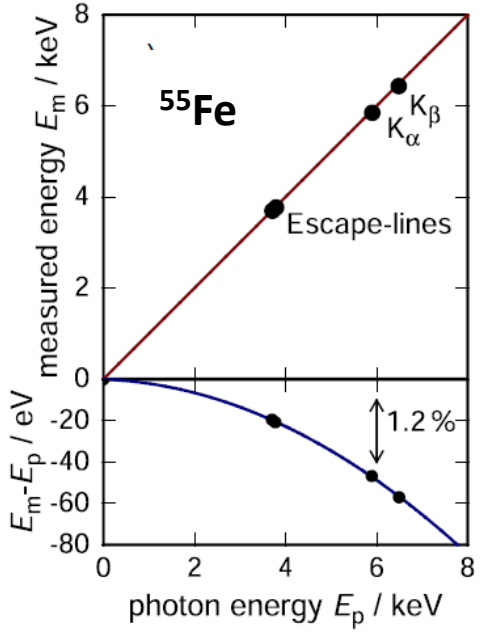

Fast risetime
→ Reduction un-resolved pile-up

Extremely good energy resolution
→ identification of small structures

Excellent linearity
→ precise definition of the energy scale

Detector geometries

- planar paramagnetic sensor
- superconducting coil
- transformed coupled to a dc SQUID

Well established:
- *superconducting meander shaped pickup loop*
- *planar sensor on top of meander-shaped coil*
- *gradiometric design*

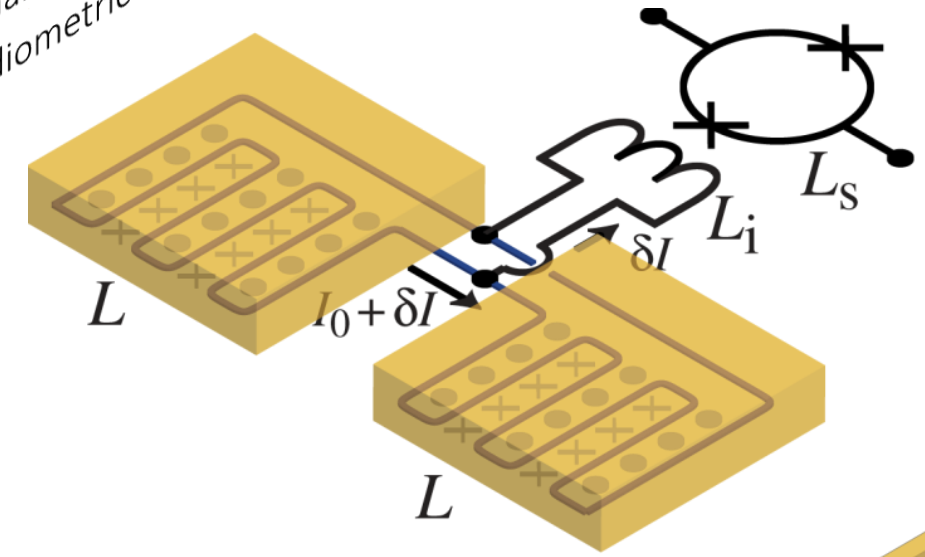

Sandwich geometry:
- *planar sensor sandwiched between stripline*
- *best magnetic flux coupling*

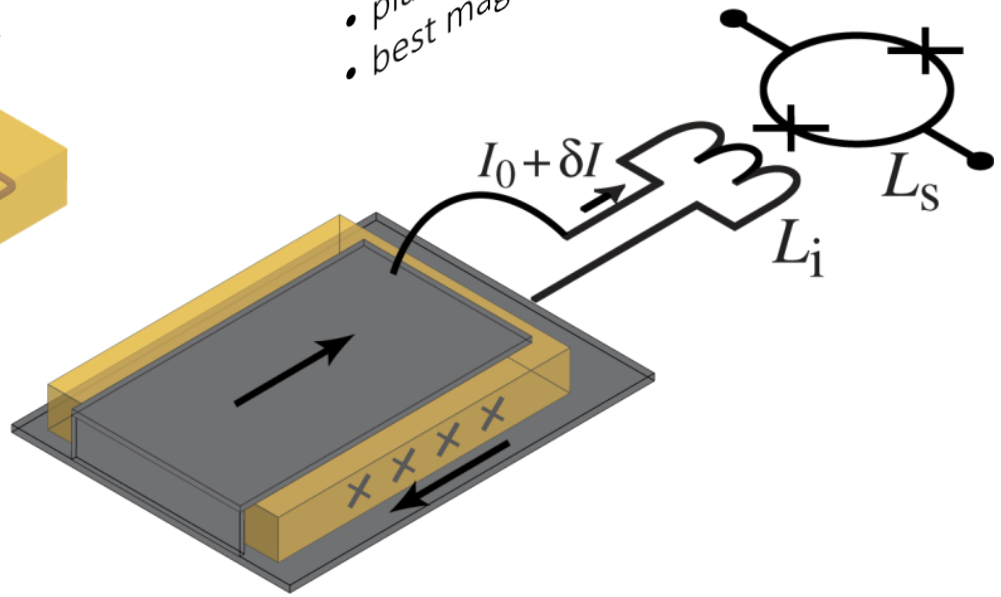

MMC readout

Two-stage dc-SQUID readout with flux-locked loop

low noise

small power dissipation on detector SQUID chip (voltage bias 1st stage)

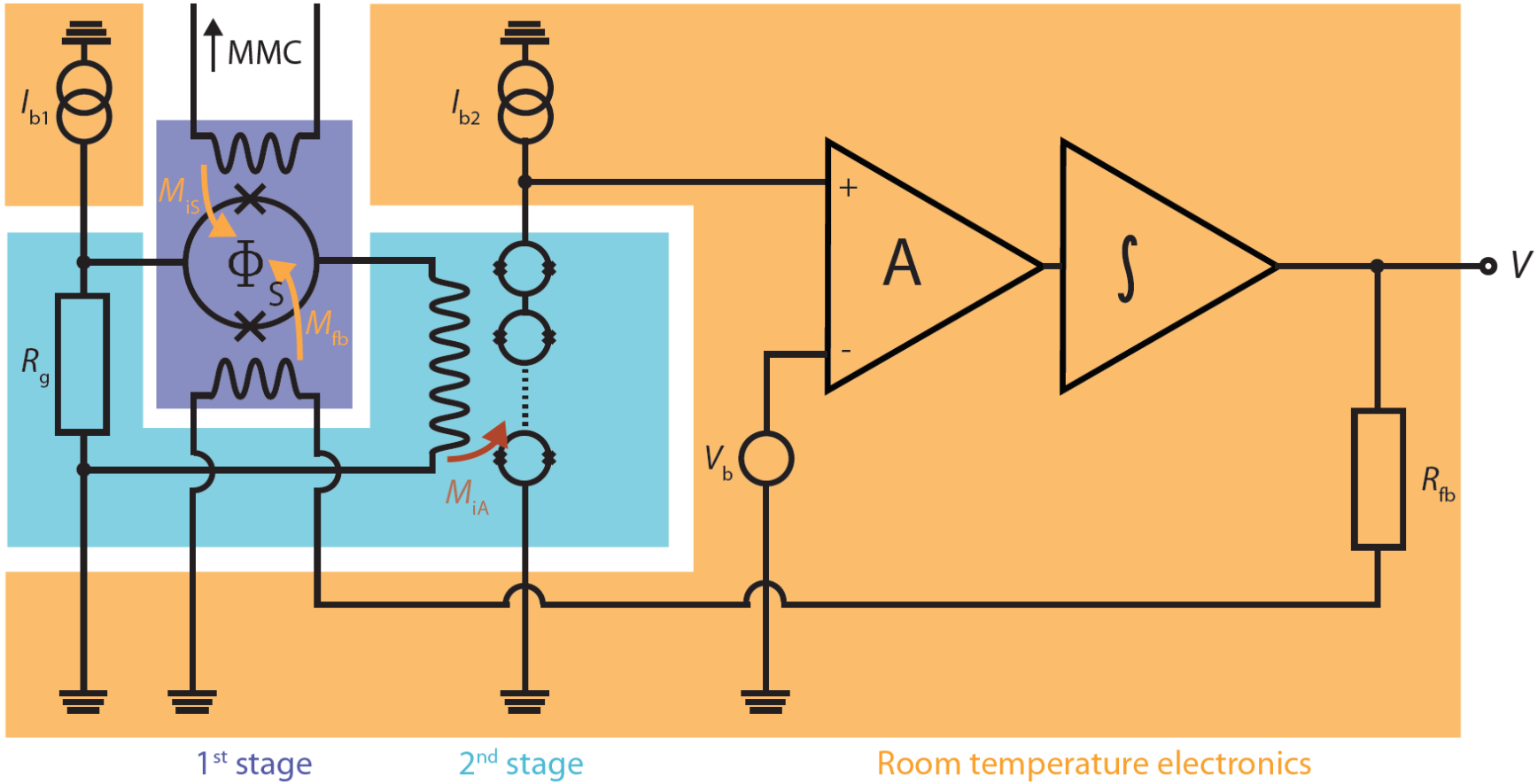

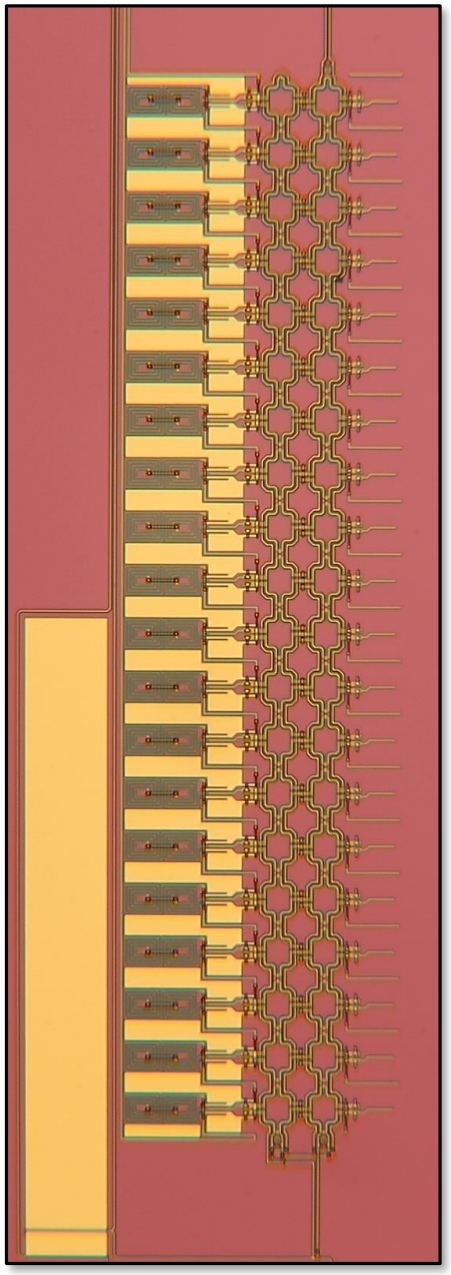

In house produced SQUID array

MMC readout

Detector module

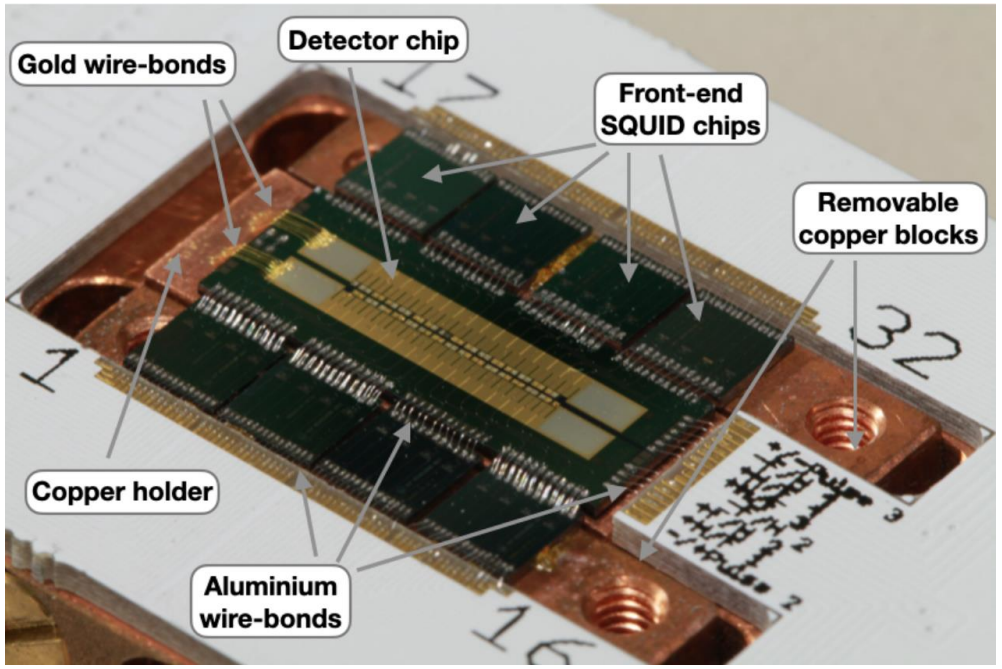

Amplifier module

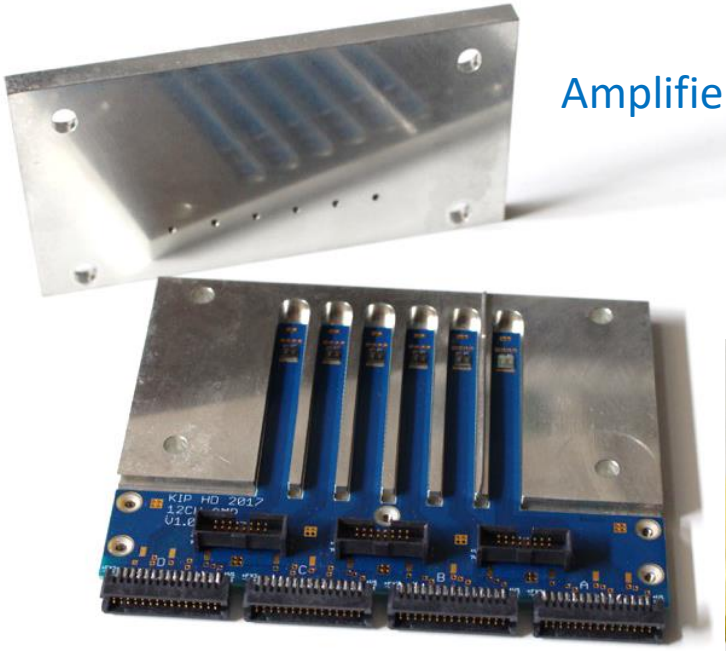

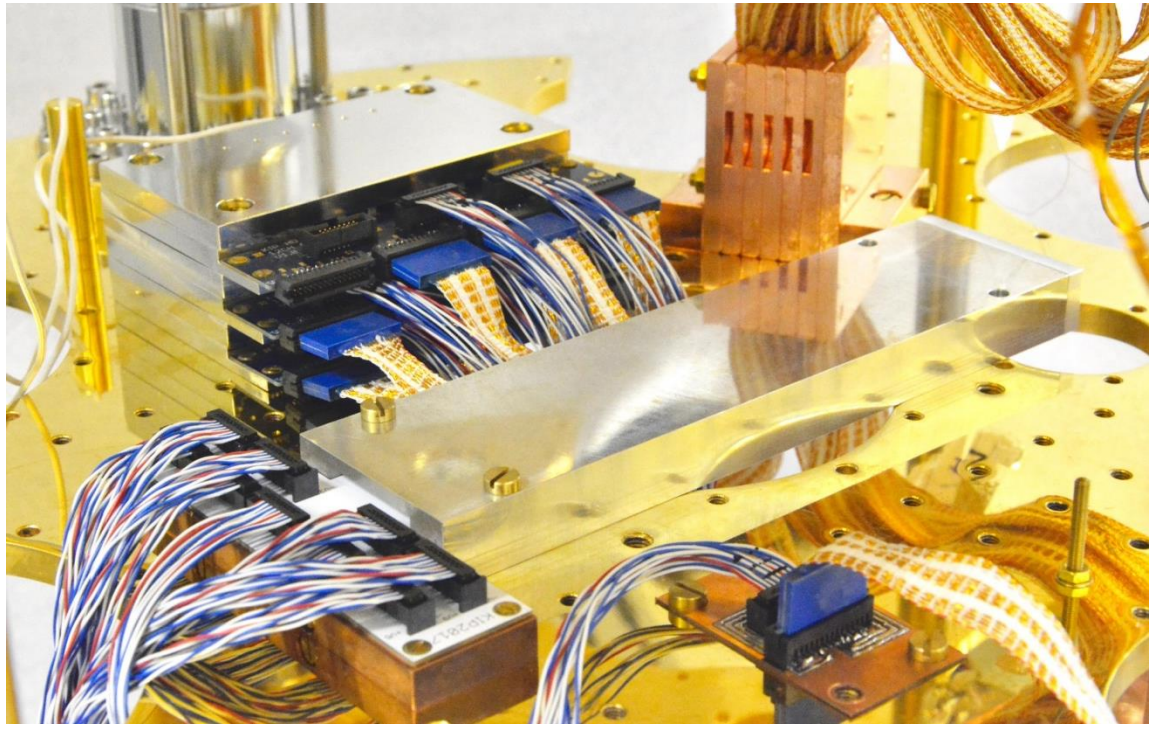

Detector and amplifier module mounted on the mixing chamber plate

F. Mantegazzini et al., *JINST* **16** (2021) P08003, arXiv:2102.11100 [physics.ins-det]

MMC readout

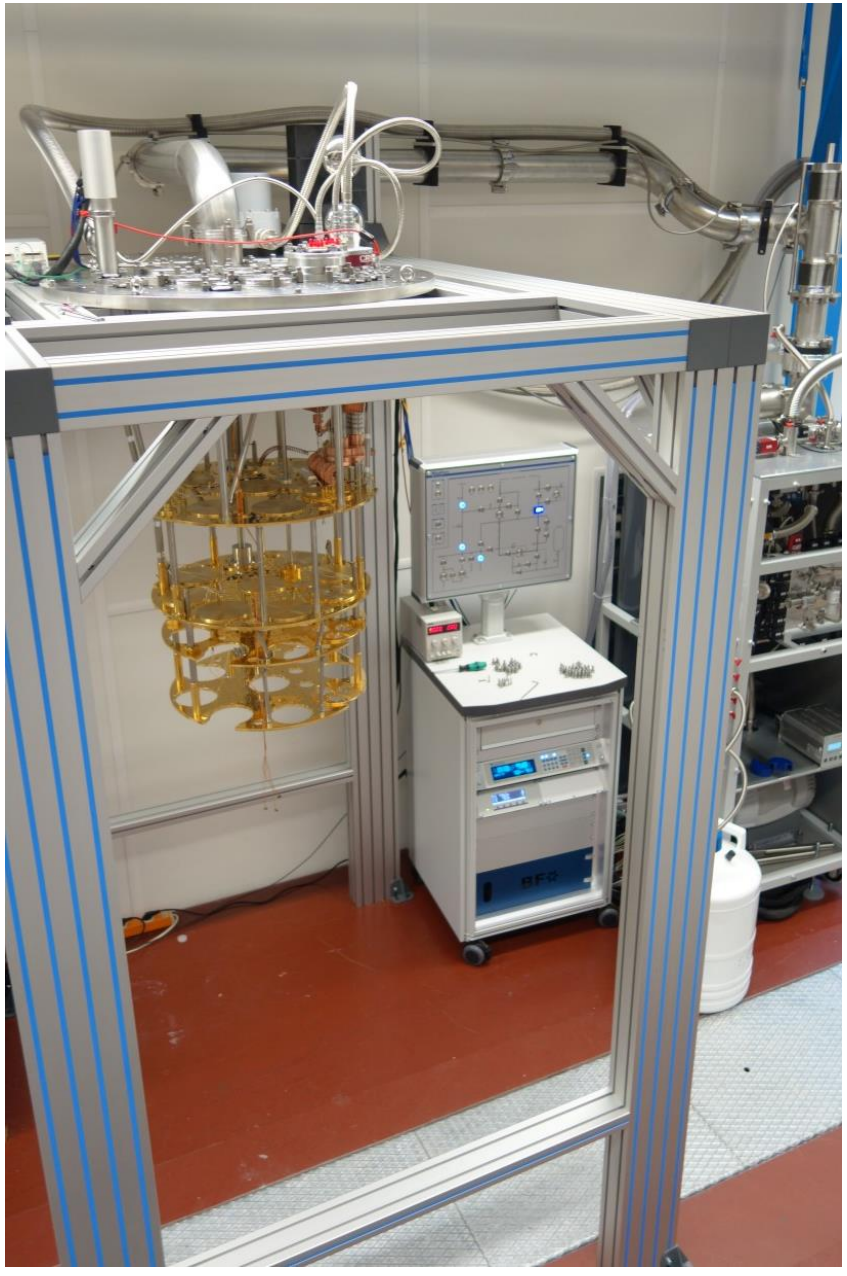

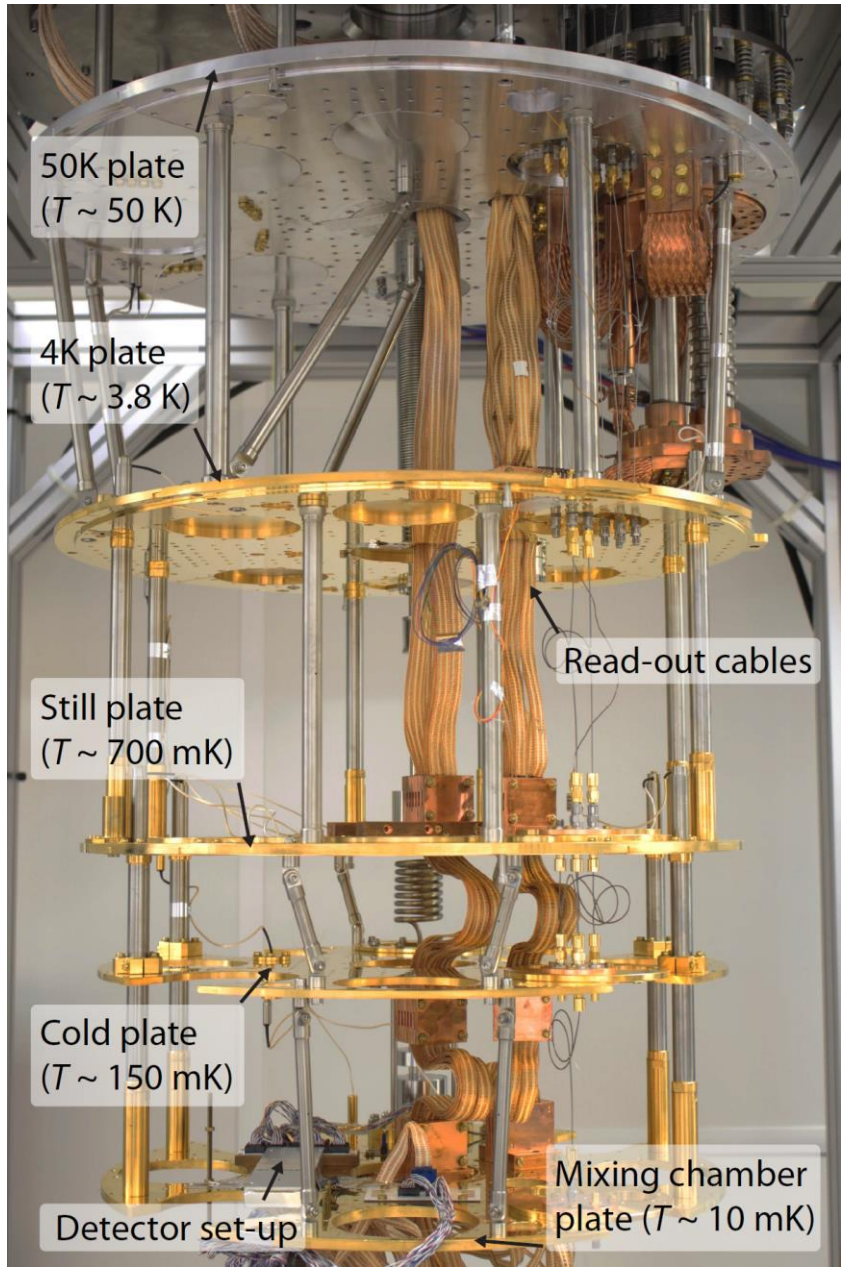
50K plate
(T ~ 50 K)
4K plate
(T ~ 3.8 K)
Read-out cables
Still plate
(T ~ 700 mK)
Cold plate
(T ~ 150 mK)
Mixing chamber
plate (T ~ 10 mK)
Detector set-up

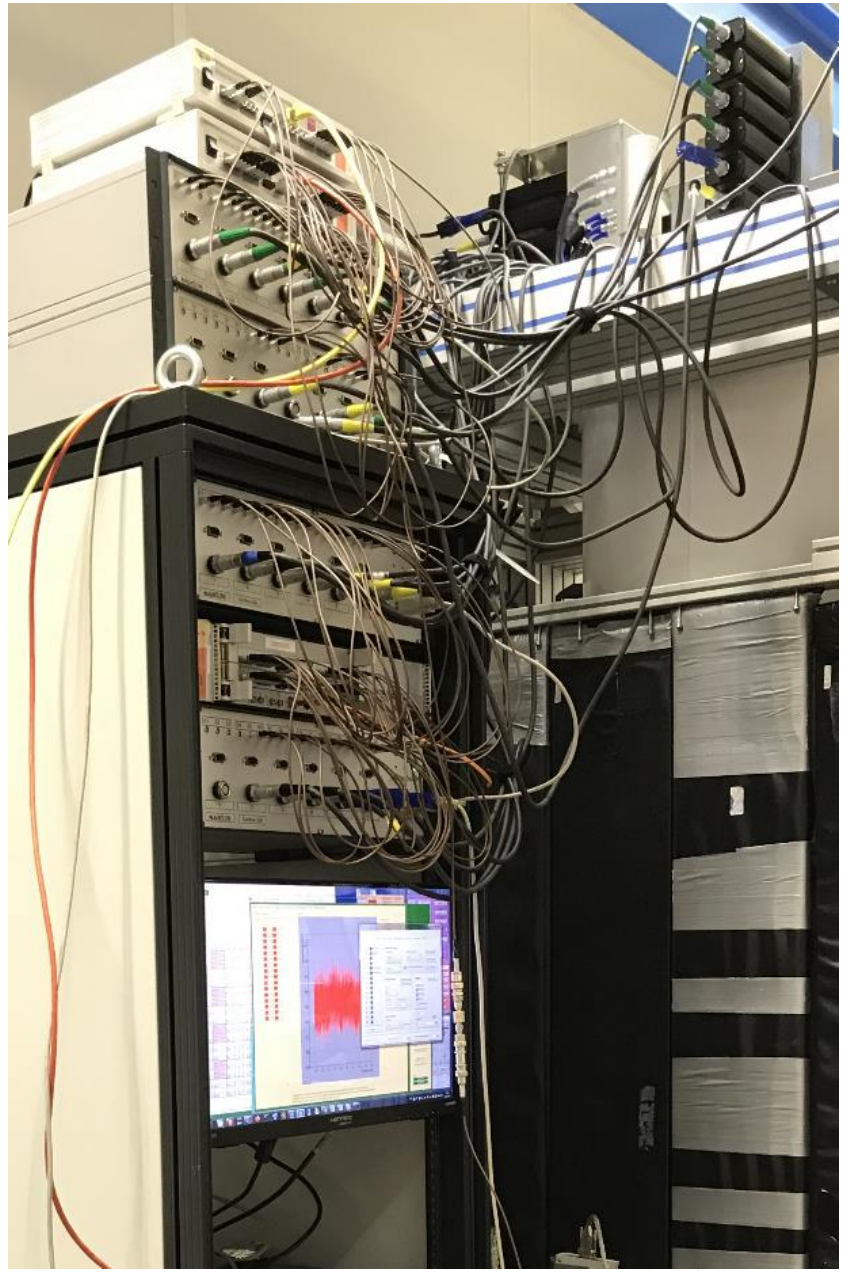

MMC fabrication

40 m^2 Cleanroom class 100
at Kirchhoff Institute for Physics

Wet bench
Chemistry bench
Maskless aligner
UHV sputtering system
Dry etching system

- Flexibility in design and fabrication
- Reliable processes for thin films
- Production of MMC array and superconducting electronics


Applications
and
Performance
Adobe Stock | #67206299

Microcalorimeter arrays for X-rays spectroscopy - maXs

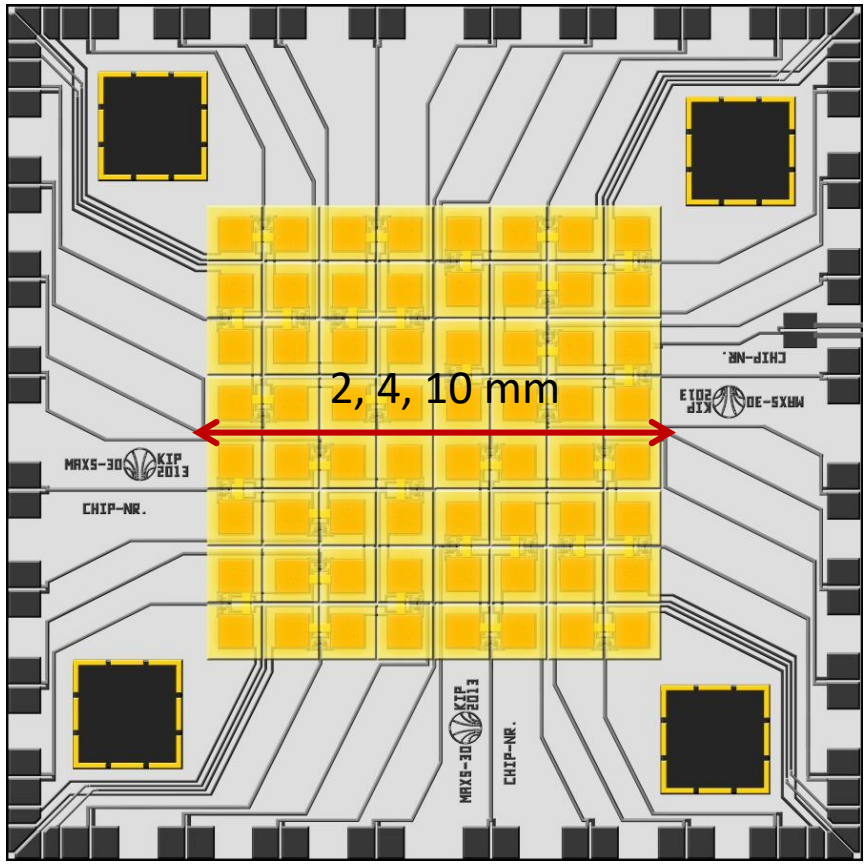

maXs-20/30/100:

- 8×8 pixels for photons up to 20/30/100 keV
- with ΔE_{FWHM} = 2/5/30 eV
- 32 two-stage dc-SQUIDs

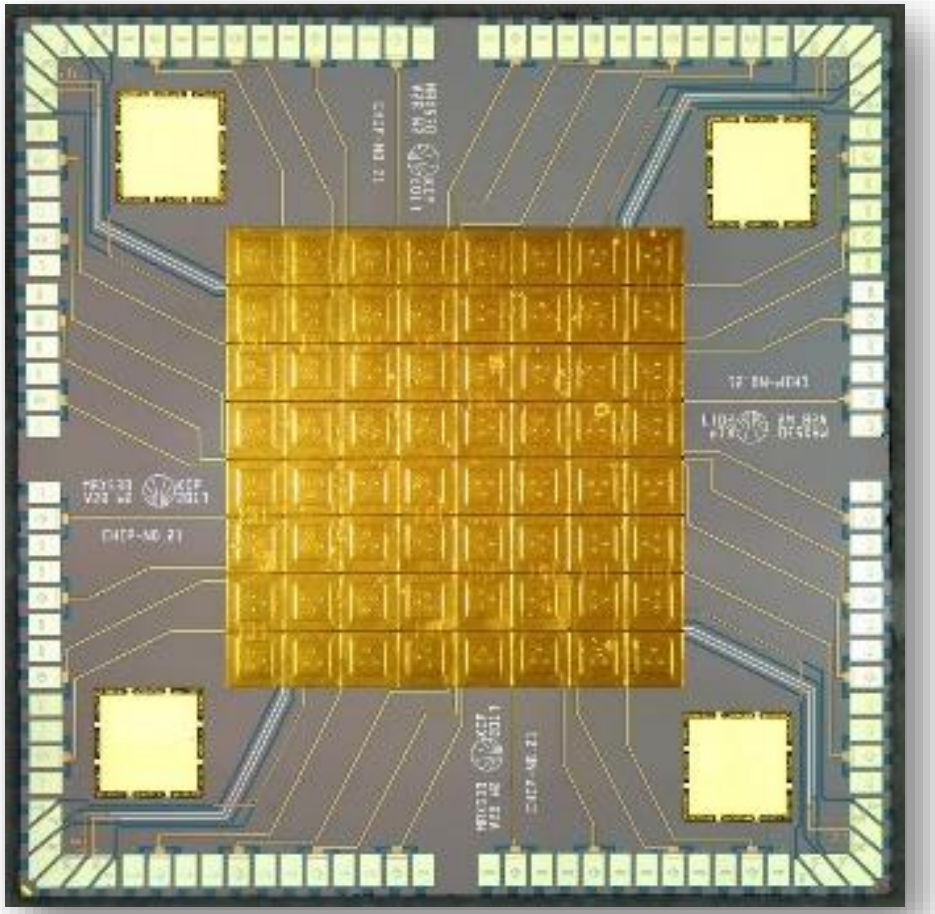

8 mm

maXs-30

Absorber size: 500 × 500 × 30 µm^3

maXs-30 set-up for IAXO

Search for an evidence for solar axions

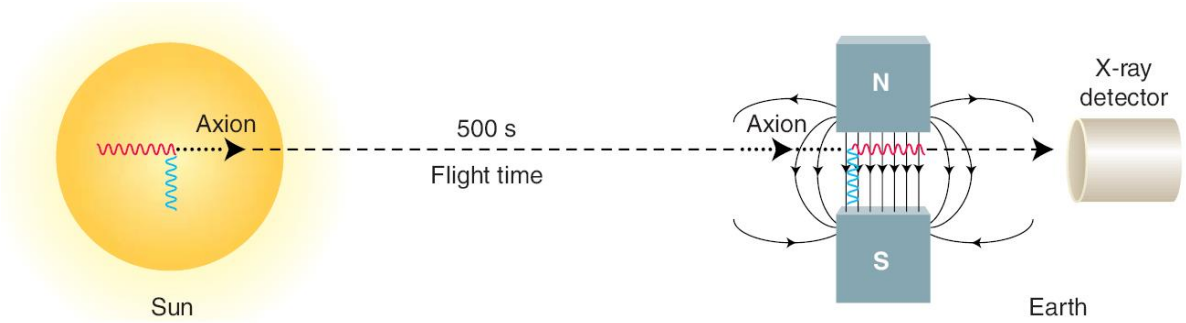

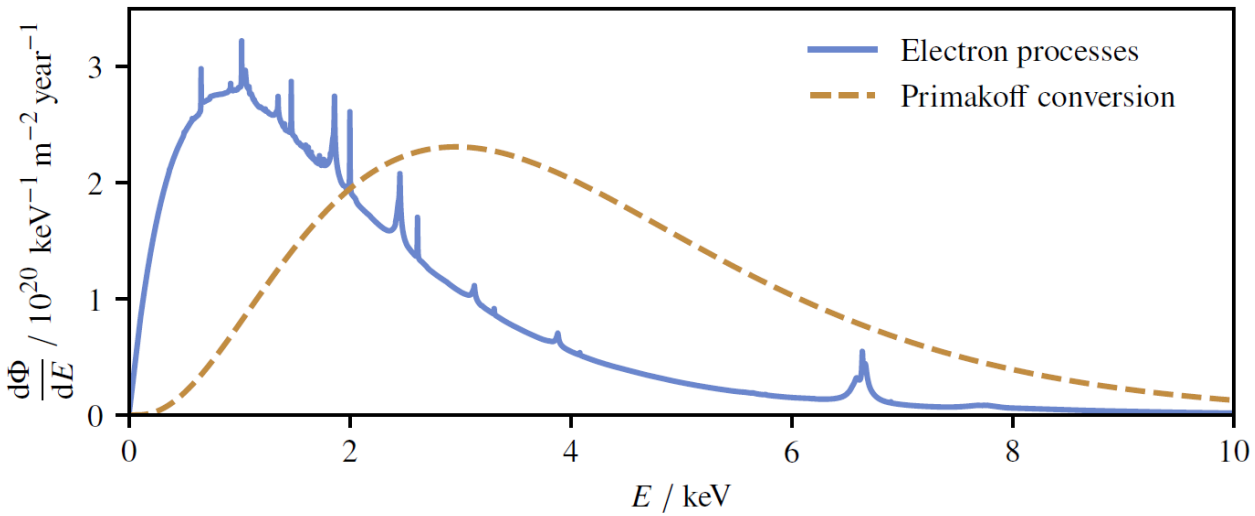

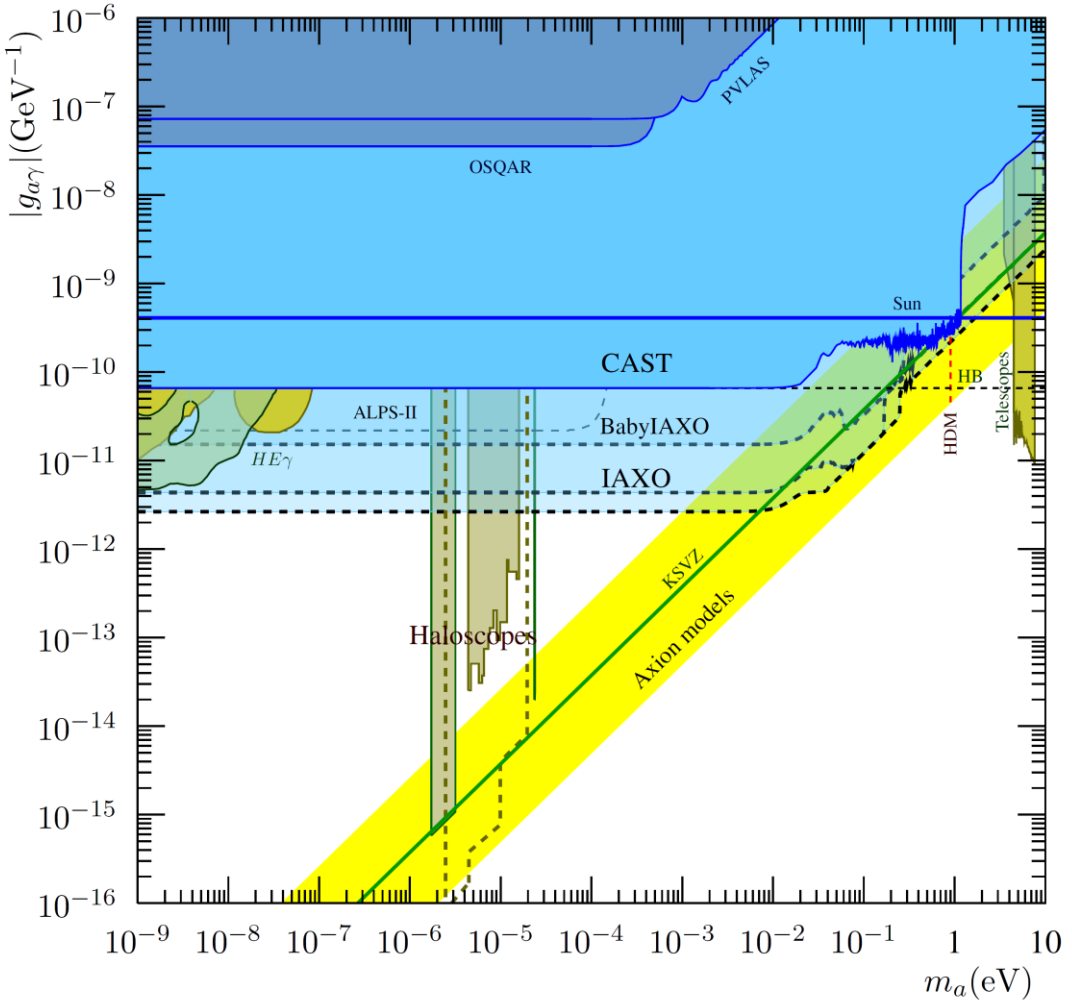

Low background and high energy resolution (low threshold) x-ray detectors

The IAXO Collaboration, *Journal of High Energy Physics* **2021** 137 (2021)

+ high energy resolution

Distinguishing Axion Models with IAXO

J. Jaeckel and L. J. Thormaehlen,
JCAP 03 (2019) 039

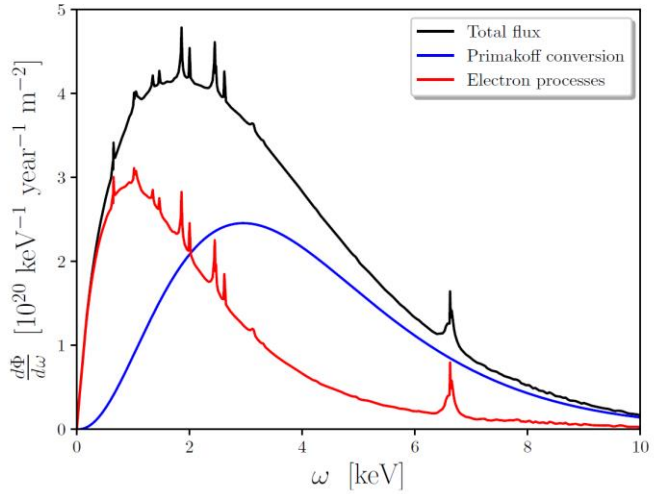

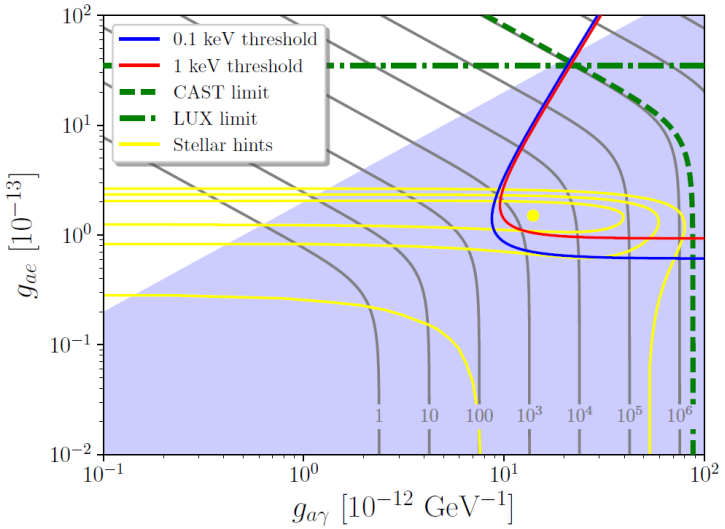

Solar metallicity

J. Jaeckel and L. J. Thormaehlen,
Phys. Rev. D 100, 123020 (2019)

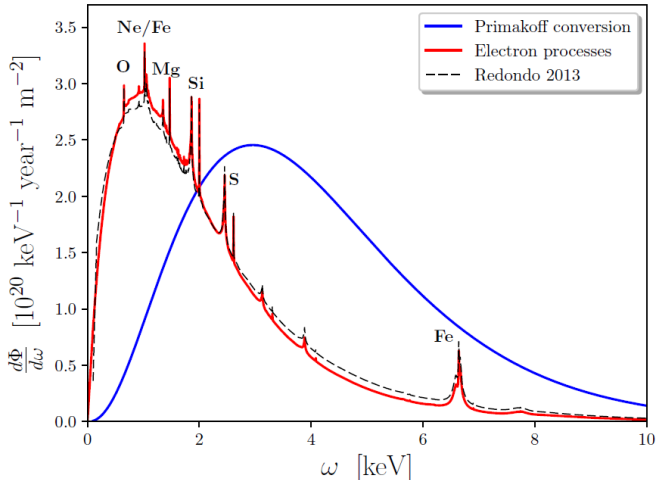

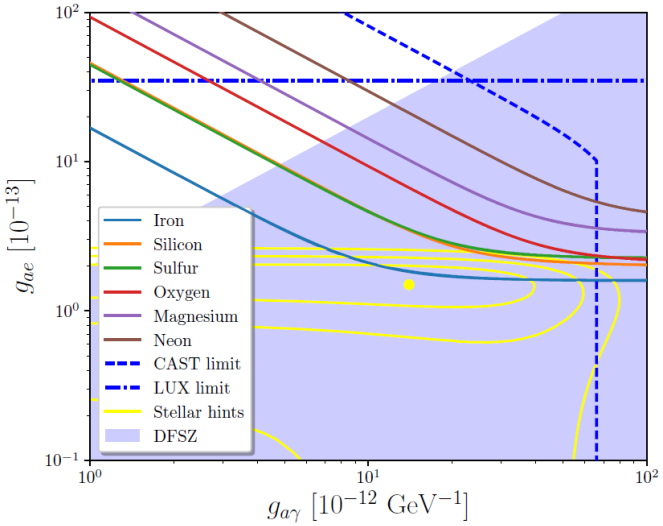

+ high energy resolution

Weighing the Solar Axion

T. Dafni et al., Phys. Rev. D 99, 035037 (2019)

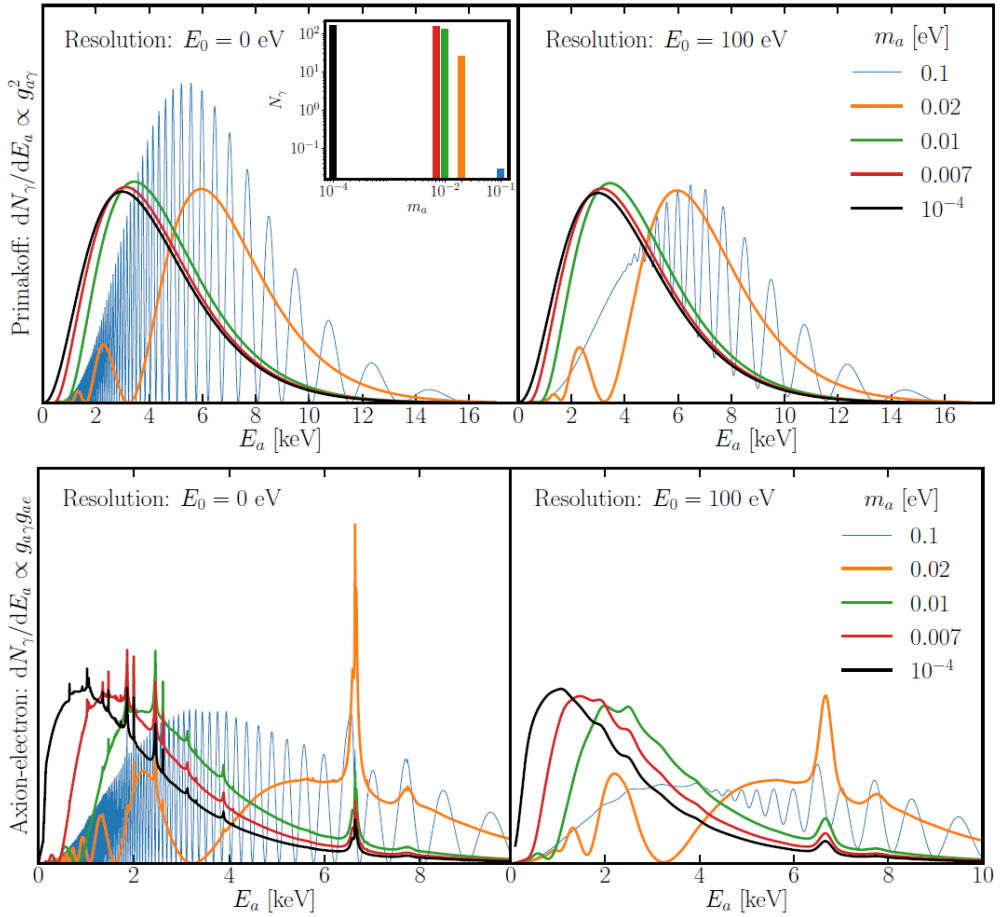

Probing the axion–nucleon coupling with the next generation of axion helioscopes

L. Di Luzio et al., EPJC 82 (2022) 120

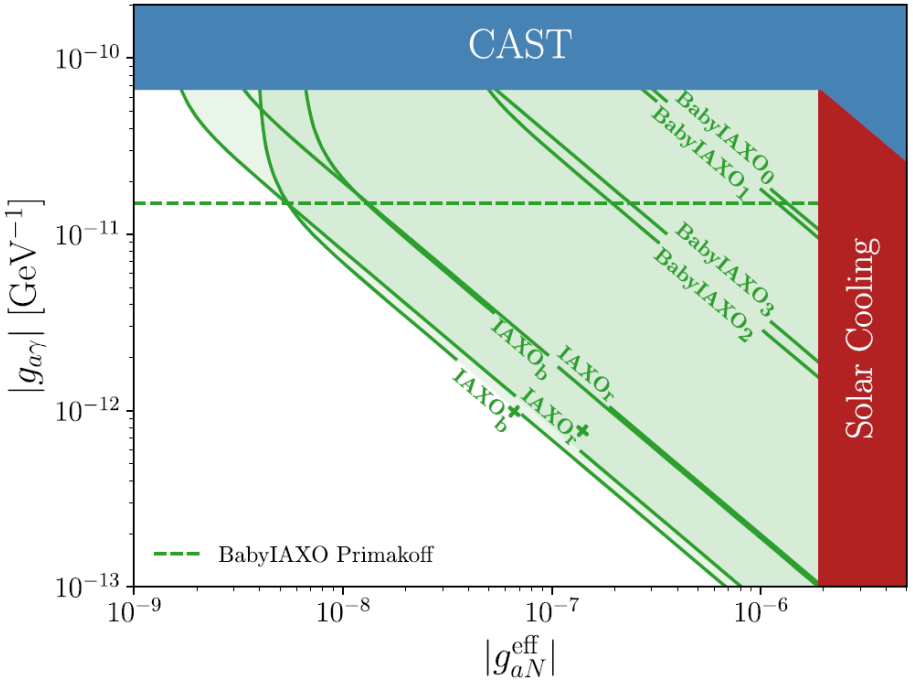

maXs-30 set-up for IAXO

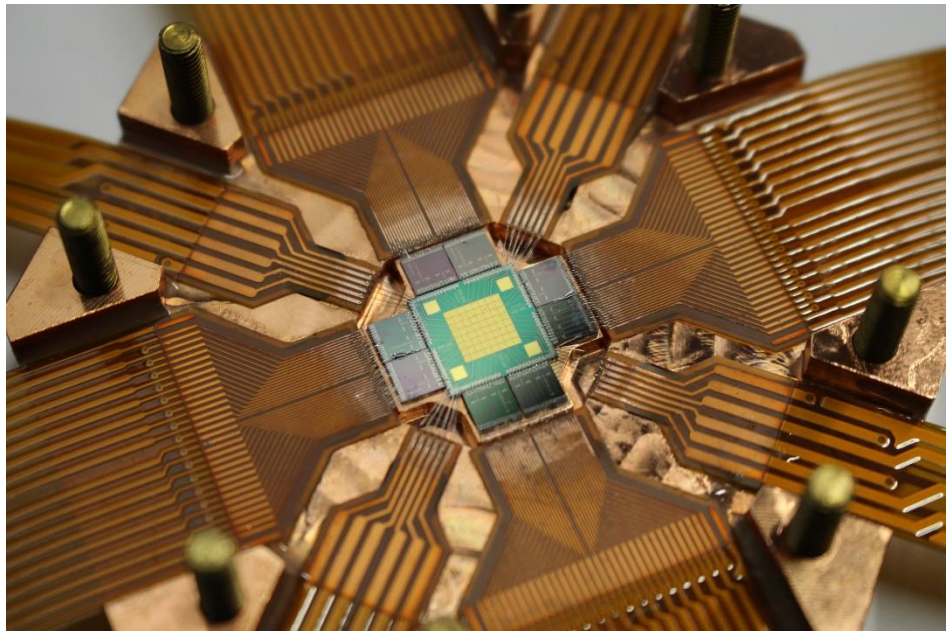

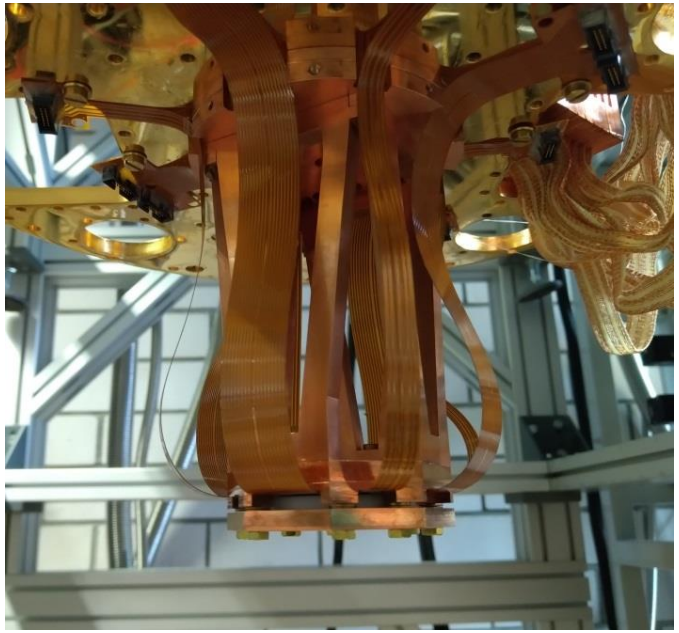

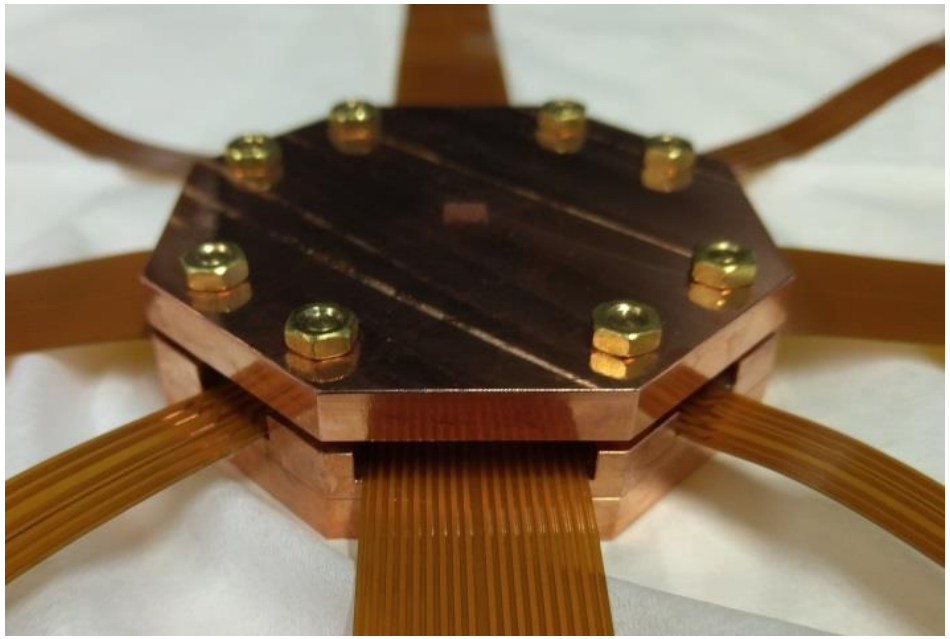

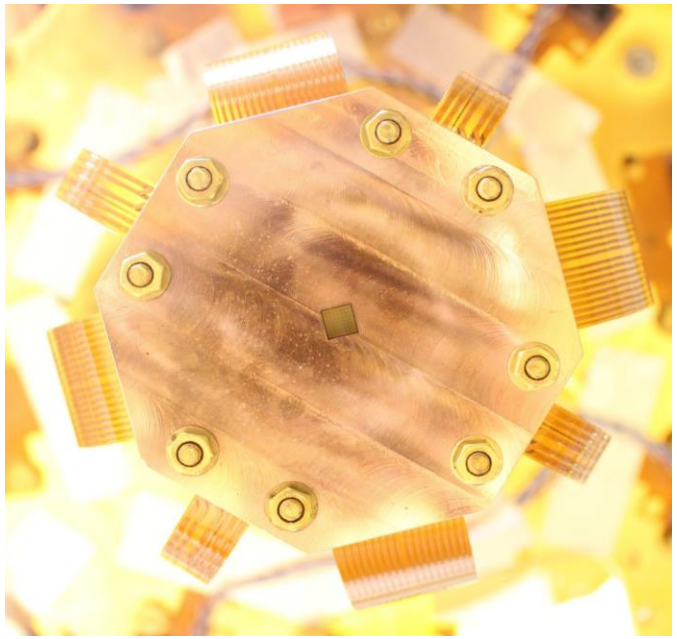

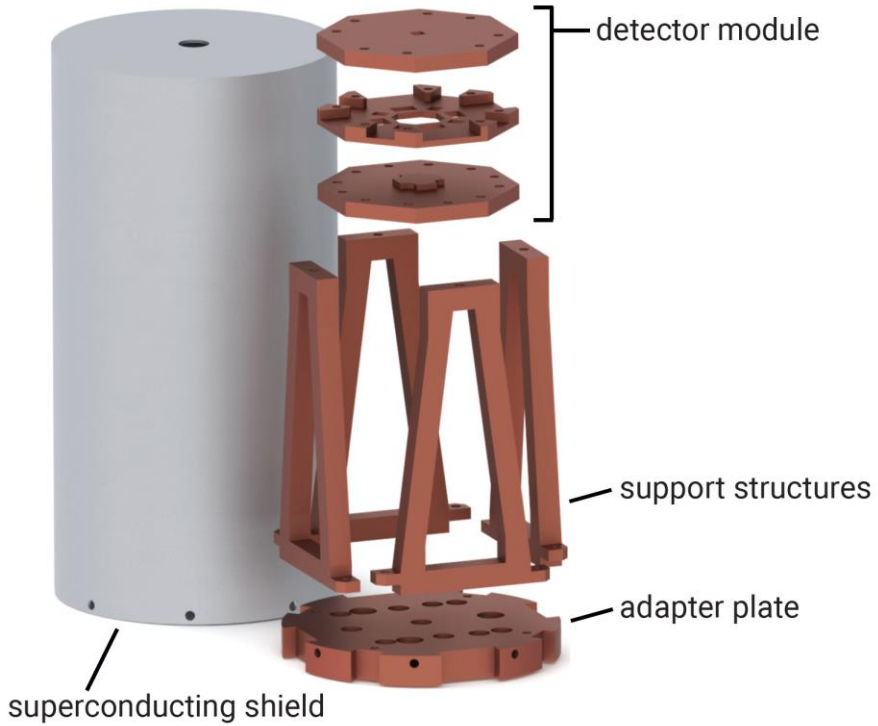

Design suitable for IAXO telescope

High purity materials for background reduction

D. Unger et al., *JINST* **16** (2021) P06006, arXiv:2010.15348 [physics.ins-det]

maXs-30 set-up for IAXO

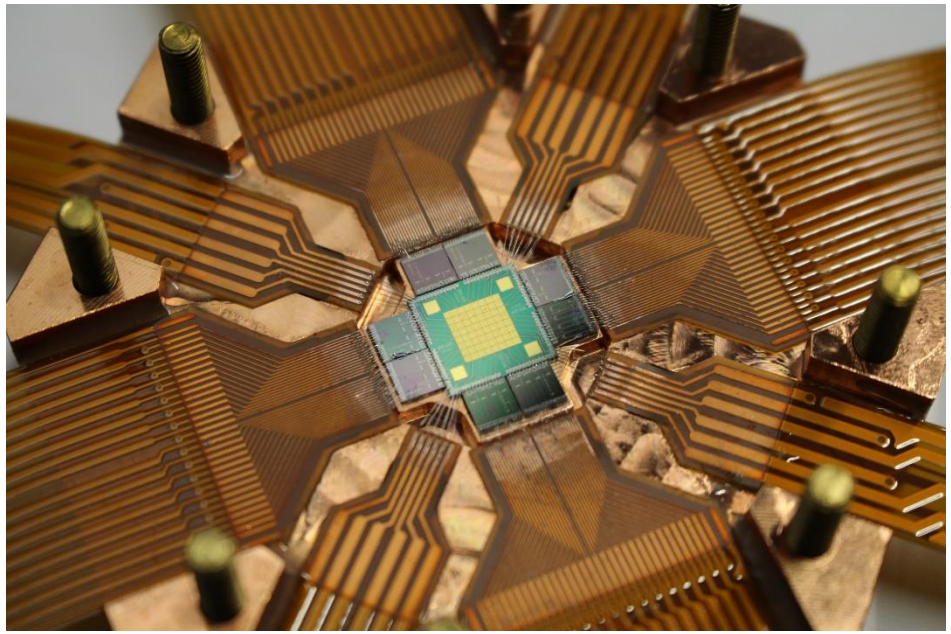

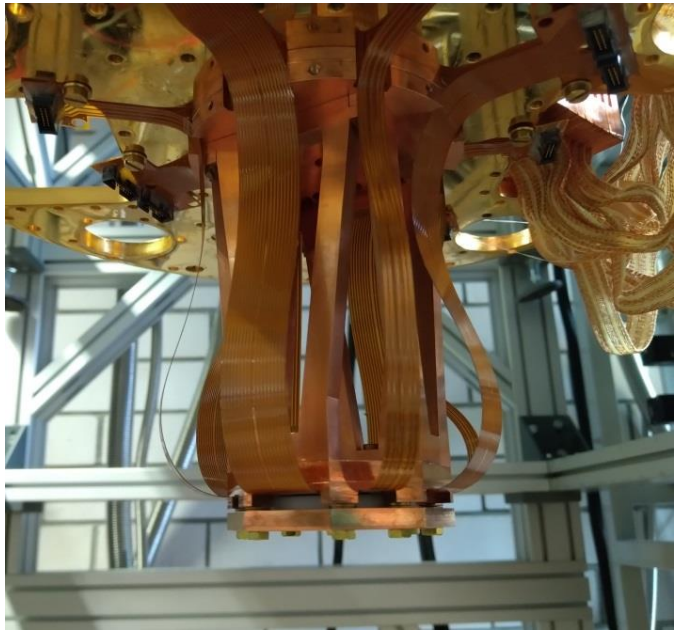

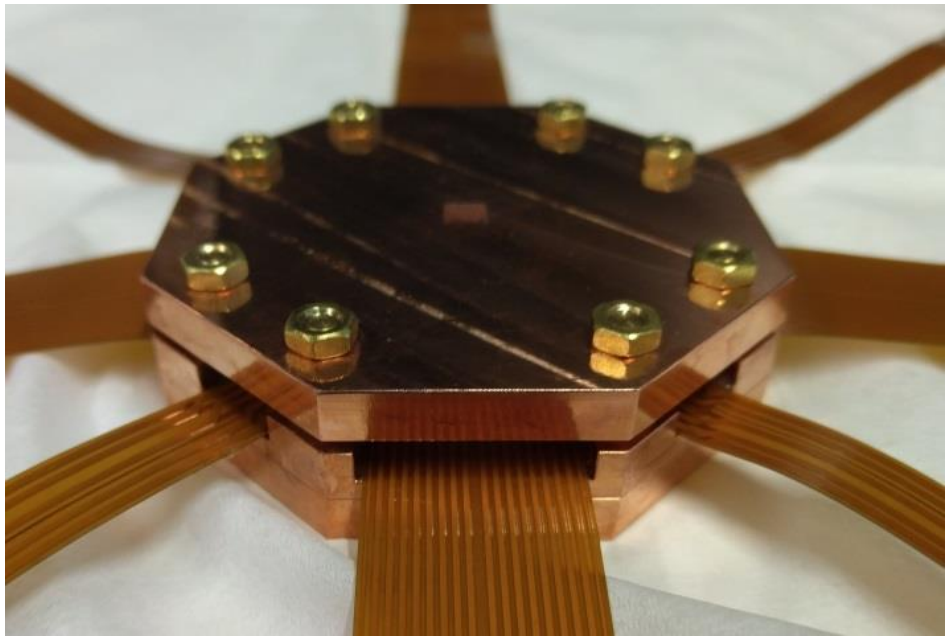

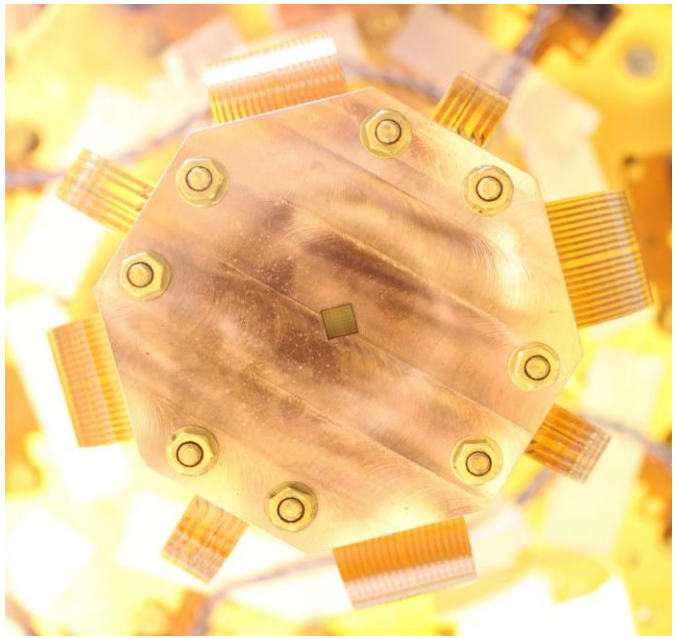

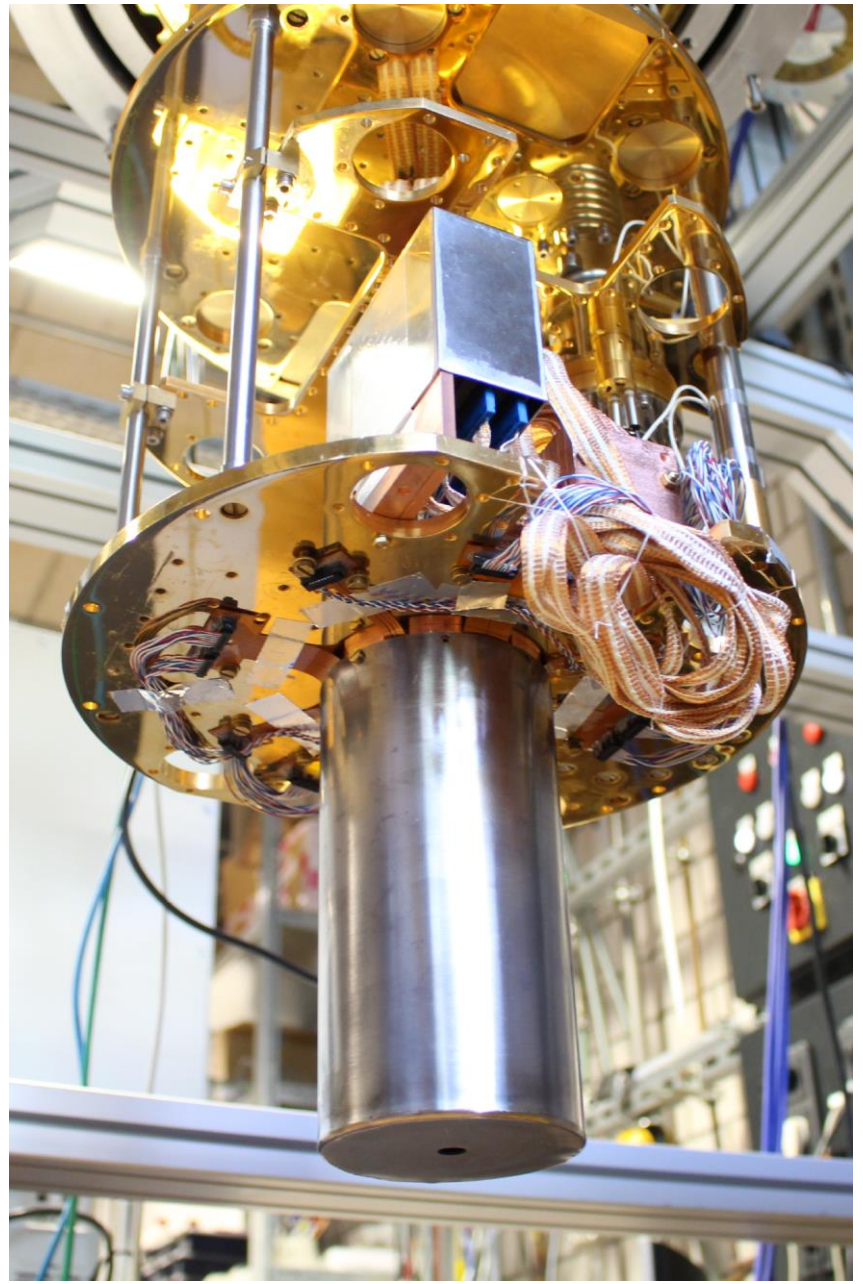

maXs-30 set-up for IAXO

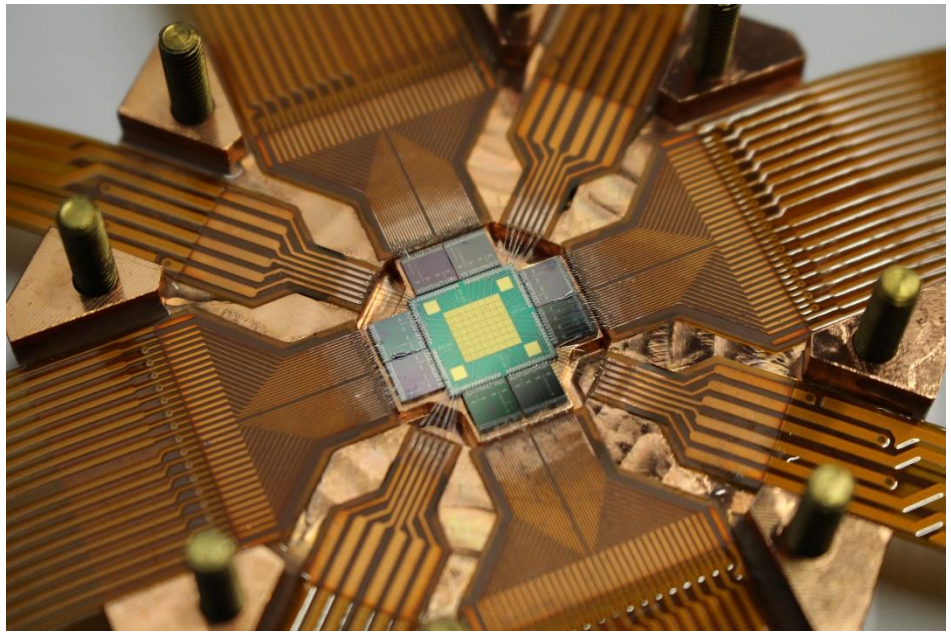

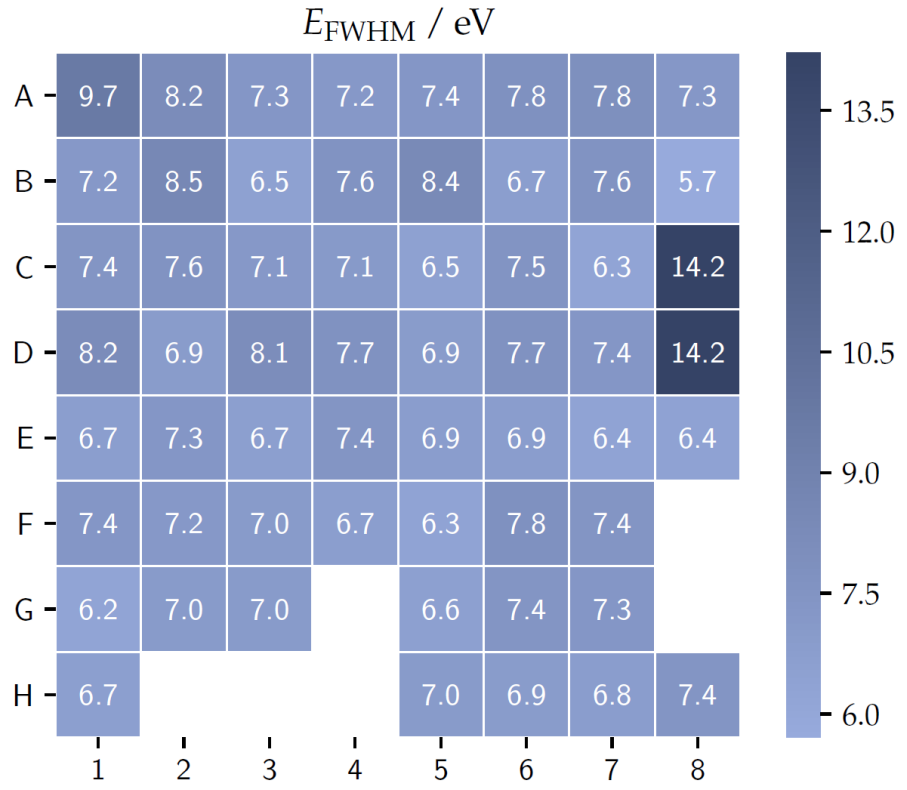

^{55}Fe calibration source
Stopping power @10 keV ~100%

- Homogeneous performance over the array
- Stable operation over 1 month

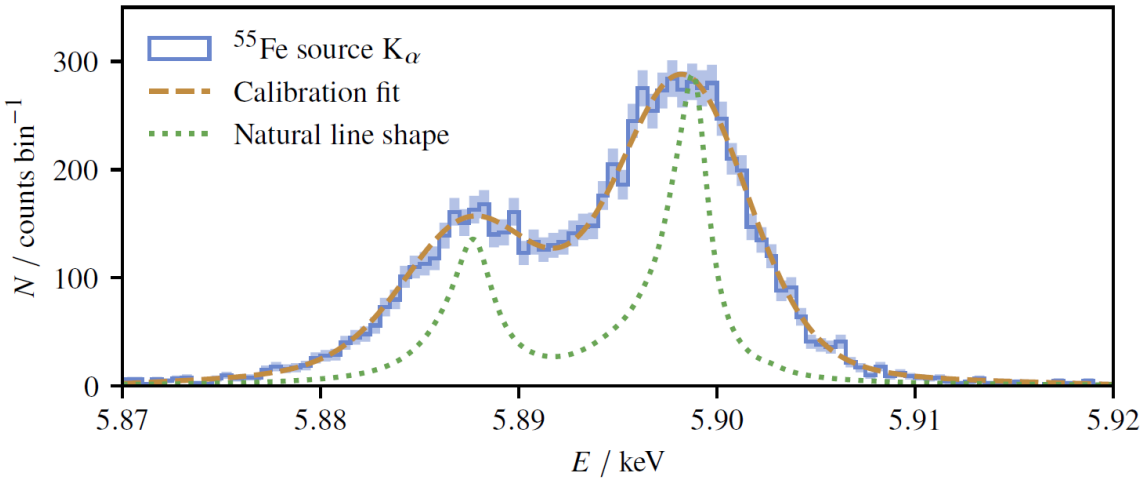

D. Unger et al., *JINST* **16** (2021) P06006,
arXiv:2010.15348 [physics.ins-det]

maXs-30 set-up for IAXO

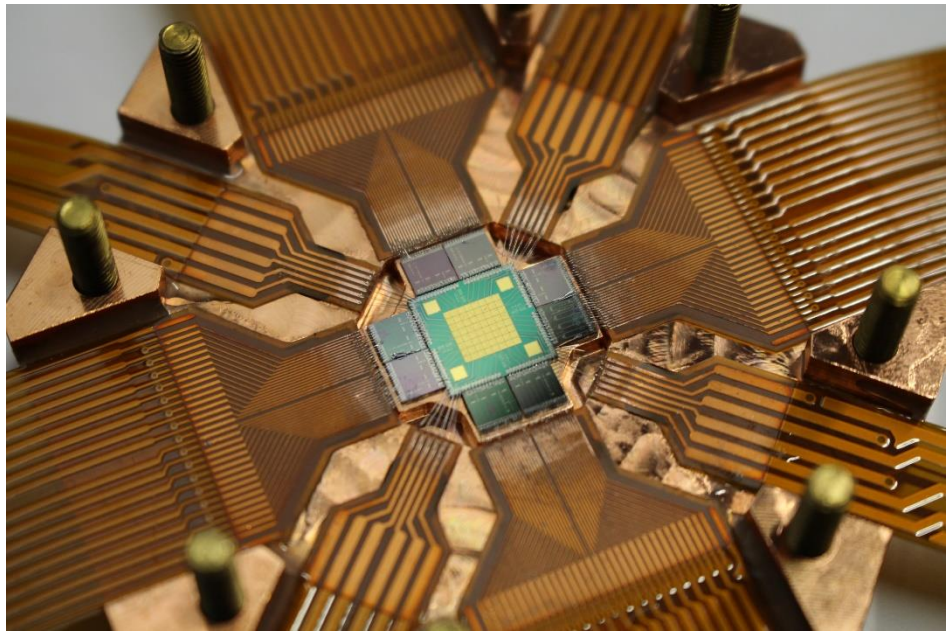

Background spectrum (one month, no special shielding, no muon veto)

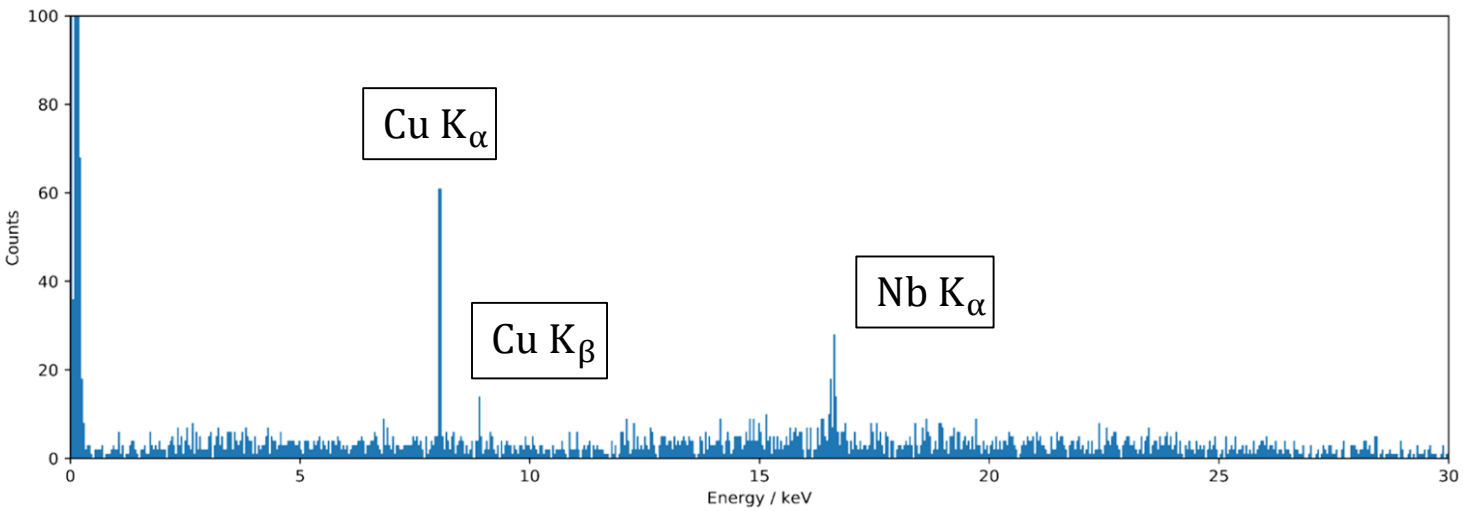

^{55}Fe calibration source
Stopping power @10 keV ~100%

- Homogeneous performance over the array
- Stable operation over 1 month

Background estimation: $2 \cdot 10^{-4} \frac{\text{counts}}{\text{keV cm}^2 \text{ s}}$
(from 1 to 10 keV)

Still too high
→ development of a cryogenic veto

D. Unger et al., *JINST* **16** (2021) P06006,
arXiv:2010.15348 [physics.ins-det]

maXs-30 with ^{241}Am + ^{233}U external sources

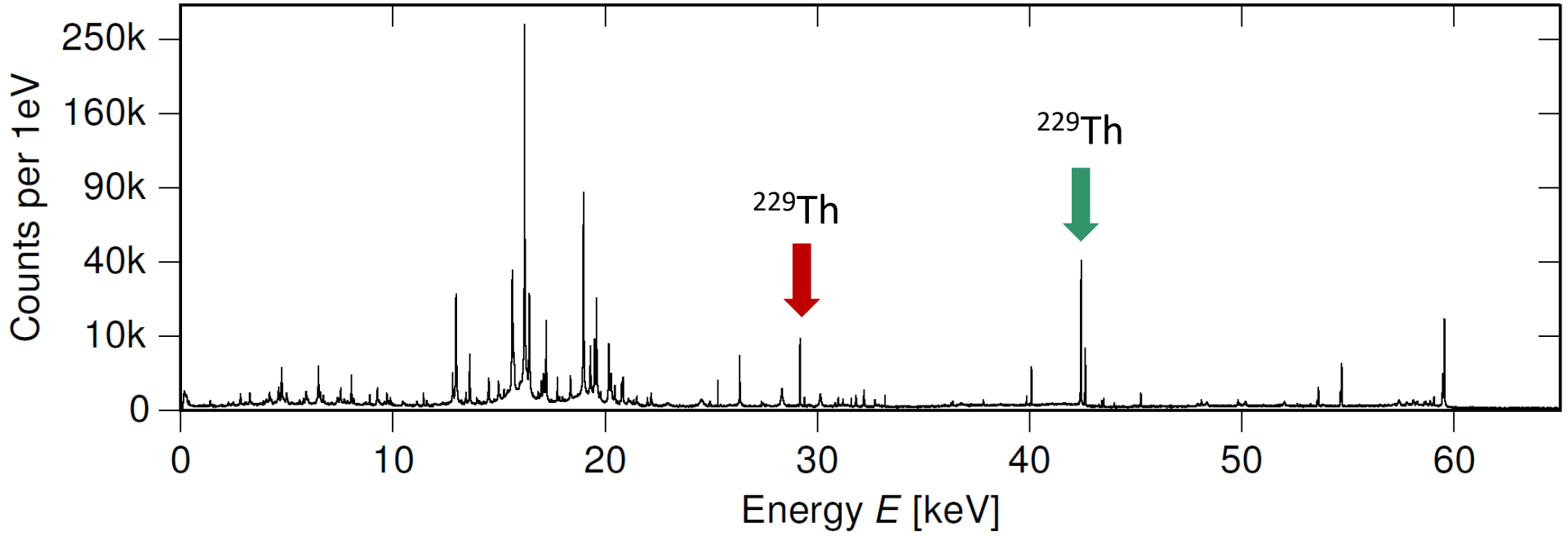

Co-added 20 channels, several weeks

T. Sikorsky et al., *Phys. Rev. Lett.* **125** (2020) 142503

maXs-30 with ^{241}Am + ^{233}U external sources

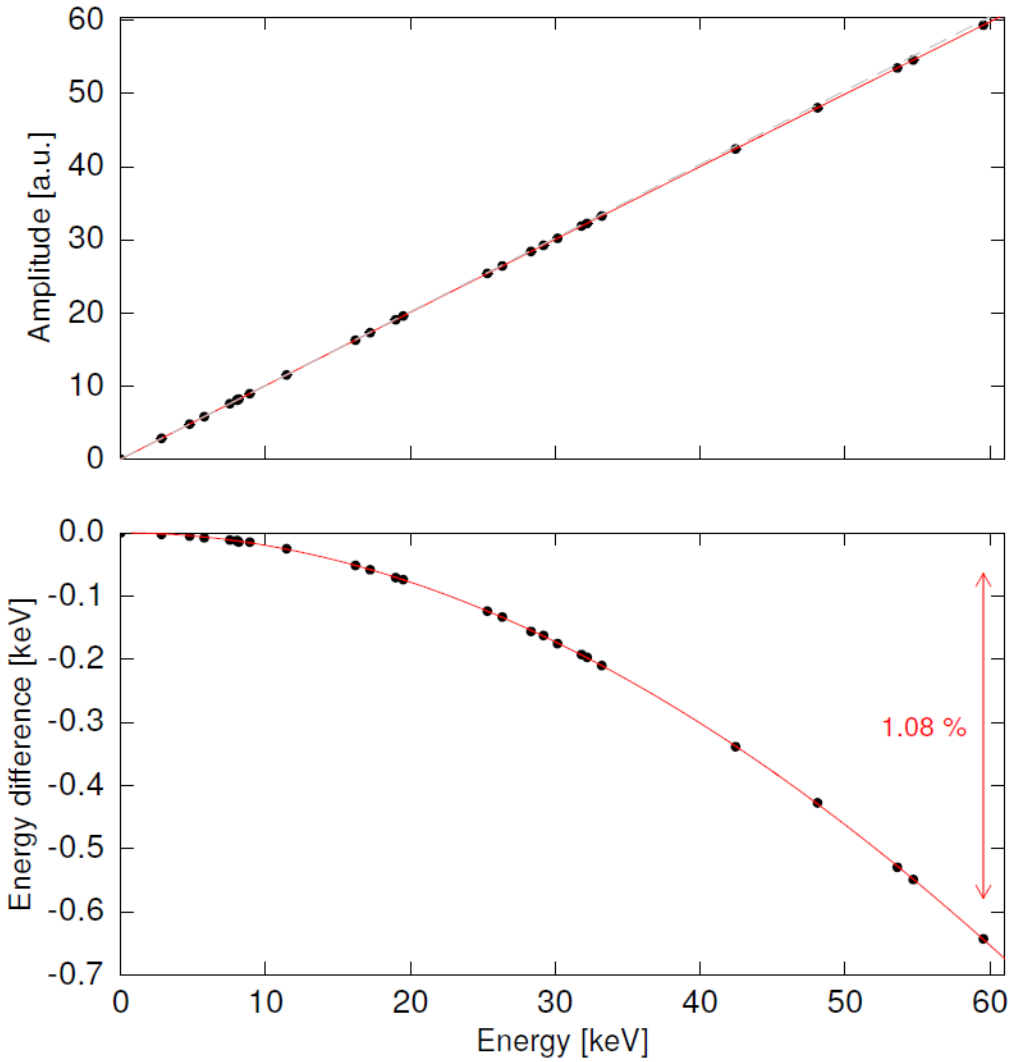

Energy calibration

- Polynomial function 2nd to 4th order
- Stable over long measuring time

non-linearity as expected from thermodynamics!

T. Sikorsky et al., *Phys. Rev. Lett.* **125** (2020) 142503

From maXs-30 to maXs-100

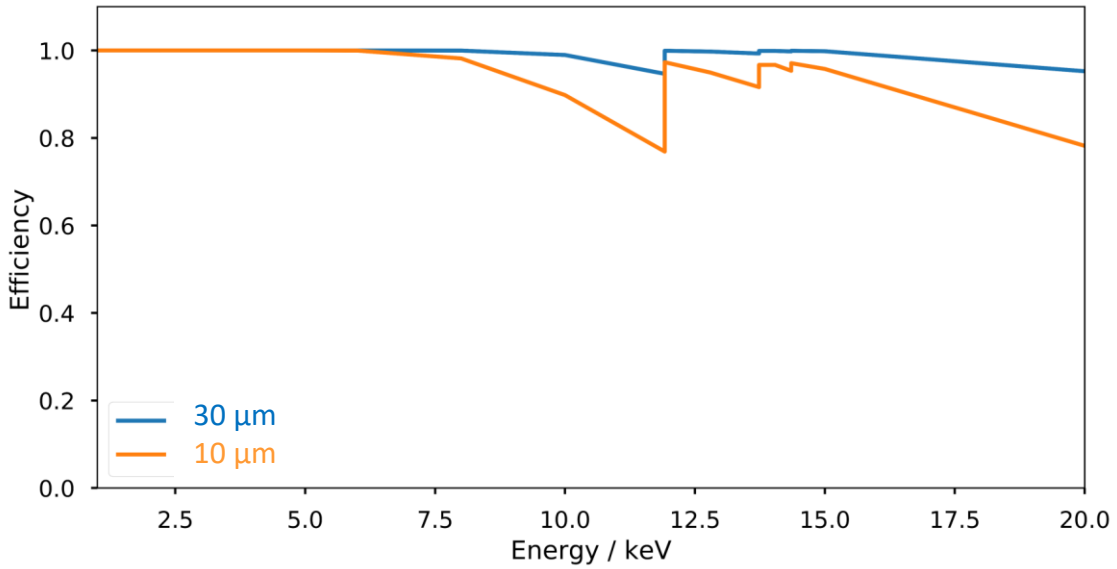

Absorber volume can be adjusted for the particles to be detected

Sensor volume is optimized to match the heat capacity of the absorber at the working temperature

Same design, but scaled up!

maXs-30

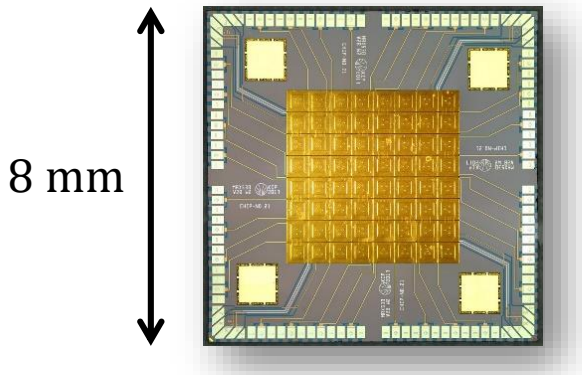

Highly charged ion spectroscopy

maXs-100

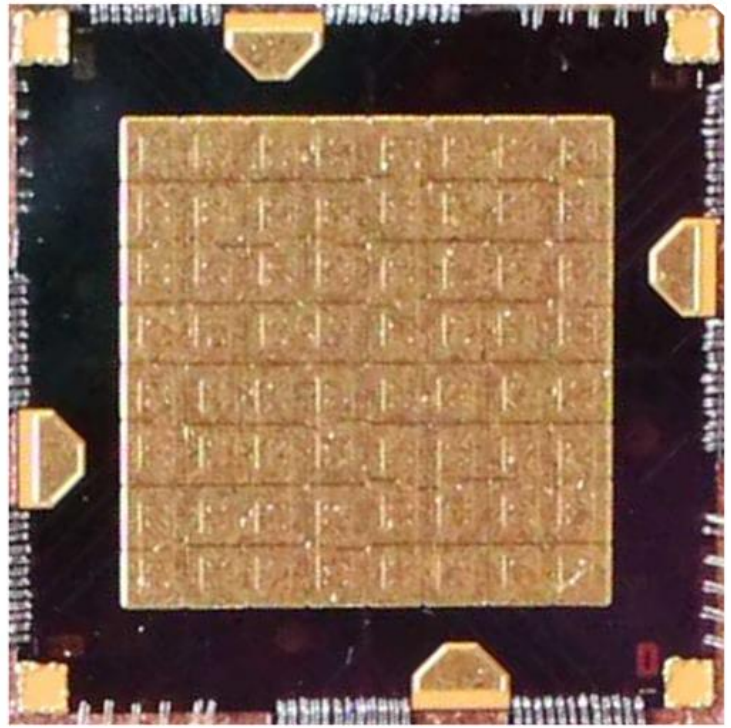

Large area/Lamb shift U^{91+}

MMCs for the ECHo experiment

ECHo uses large arrays of MMCs with enclosed ^{163}Ho

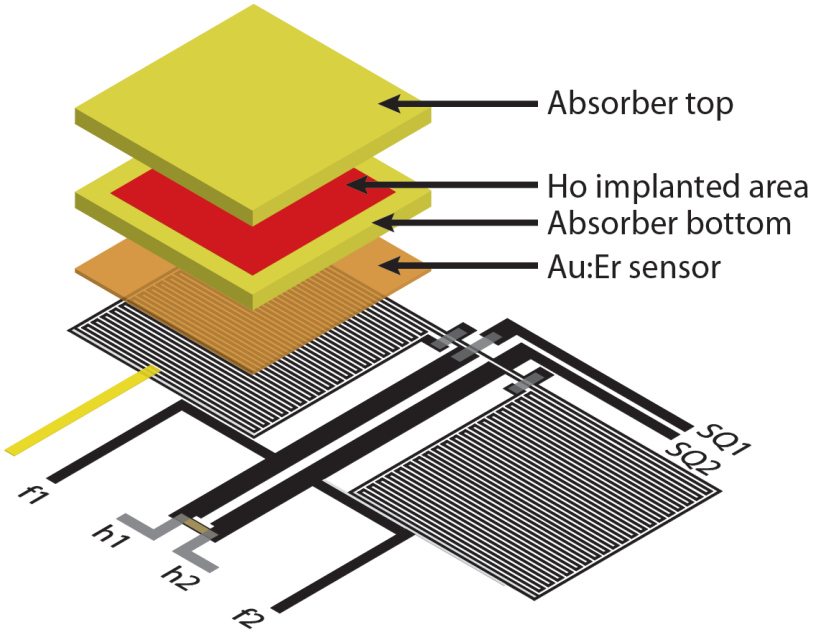

Implantation square:
150 µm x 150 µm

Second absorber:
165 µm x 165 µm

First absorber:
180 µm x 180 µm

Fraction of events
in the last eV ~10^{-12}

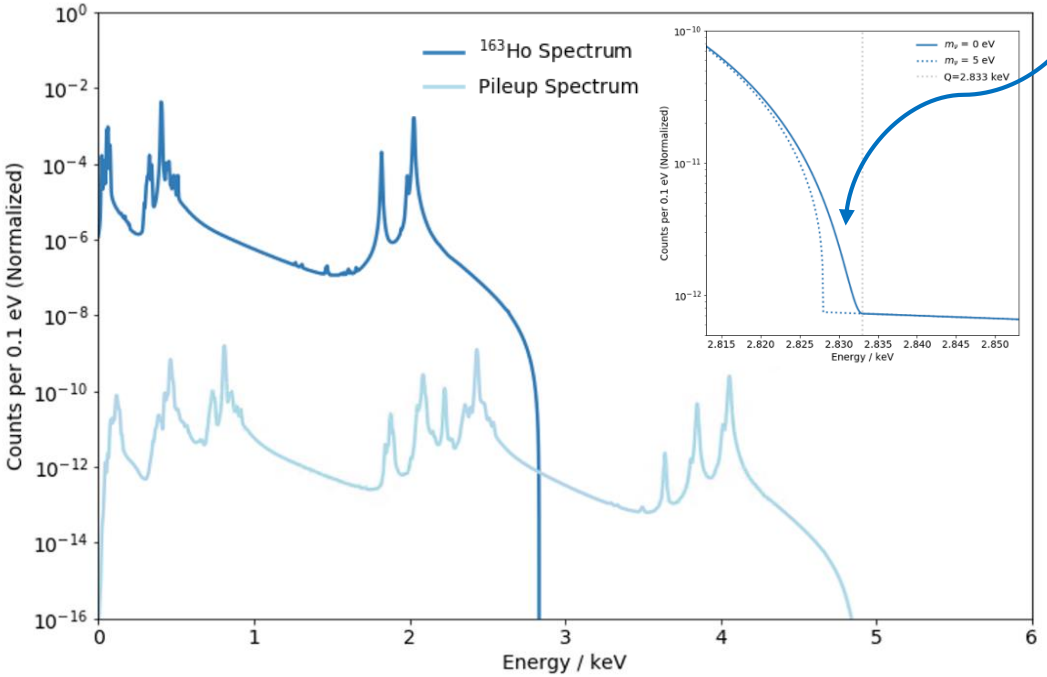

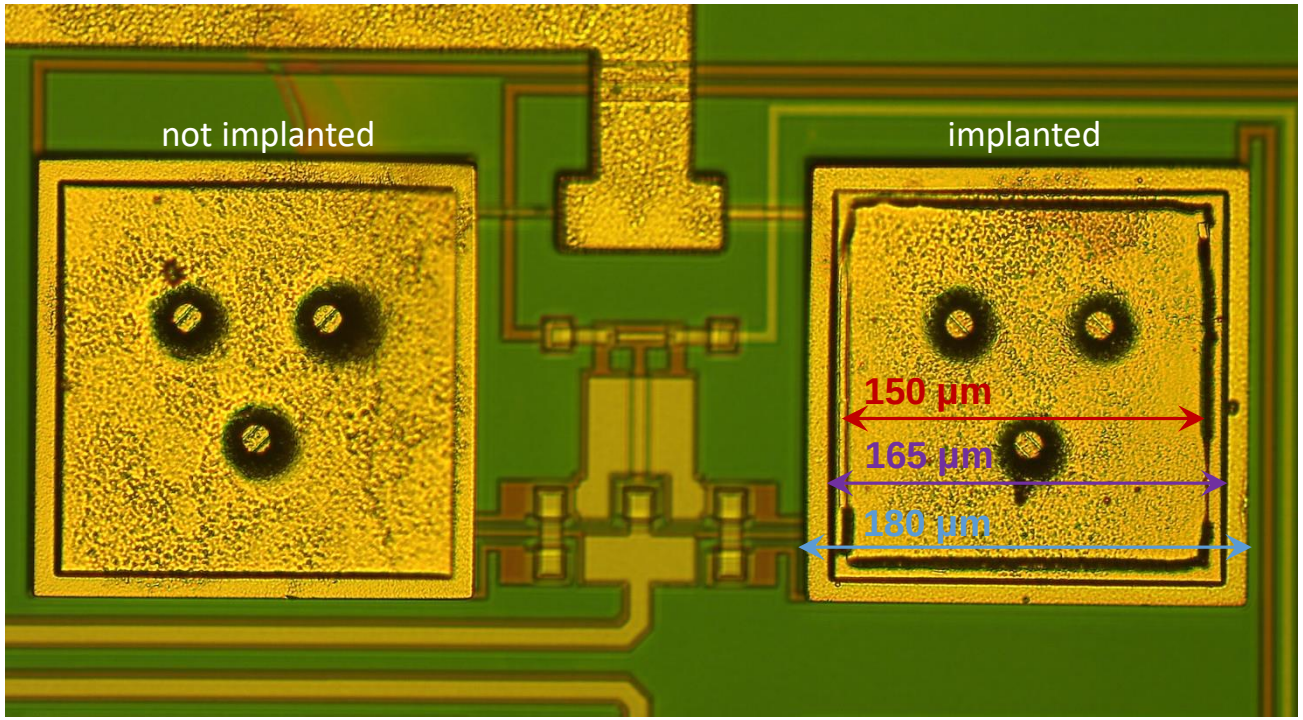

M. Braß and M. W. Haverkort, *New J. Phys.* **22** (2020) 093018

ECHo-1k array

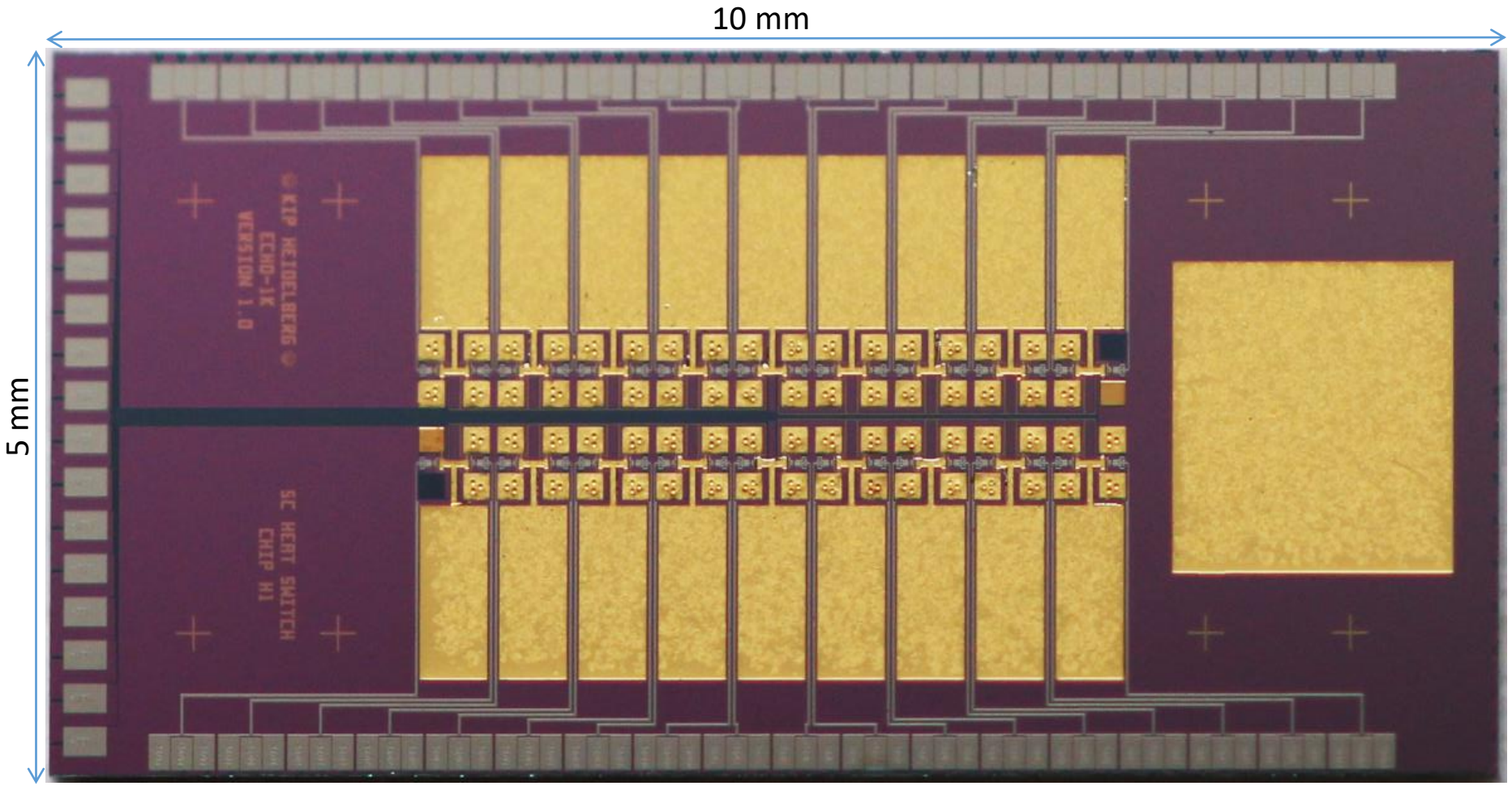

64 pixels can be loaded with ^{163}Ho
+ 2 temperature pixels
+ 2 detectors for diagnostics

Design performance:
ΔE_{FWHM} ~ 5 eV
τ_r ~ 90 ns (single channel readout)

F. Mantegazzini et al., NIM A, Vol. 1030, 2022, 166406

ECHo-1k array

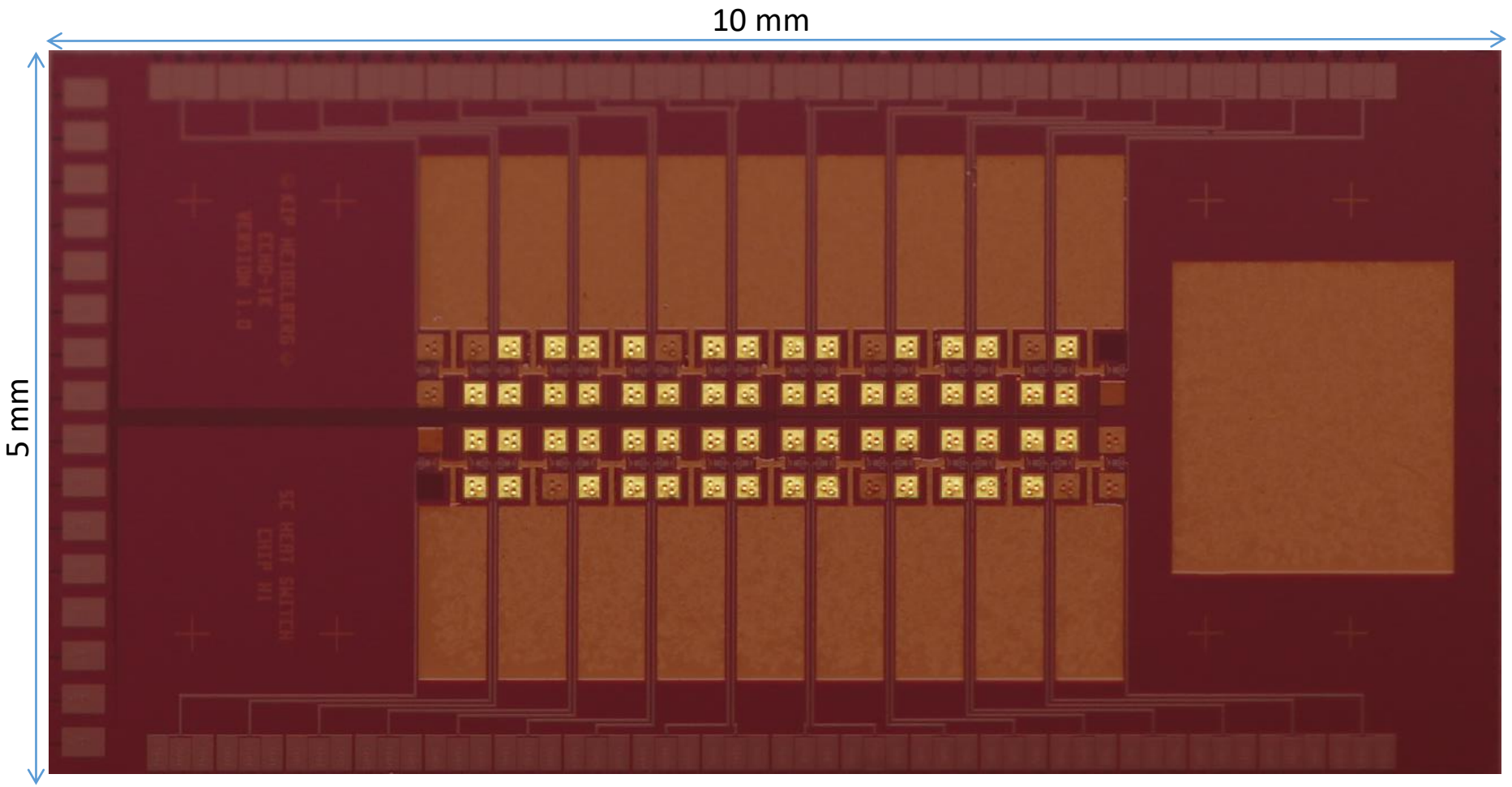

64 pixels can be loaded with ^{163}Ho
+ 2 temperature pixels
+ 2 detectors for diagnostics

Design performance:
ΔE_{FWHM} ~ 5 eV
τ_r ~ 90 ns (single channel readout)

✓ presence of non-implanted chips for in-situ background determination

F. Mantegazzini et al., NIM A, Vol. 1030, 2022, 166406

ECHo-1k readout

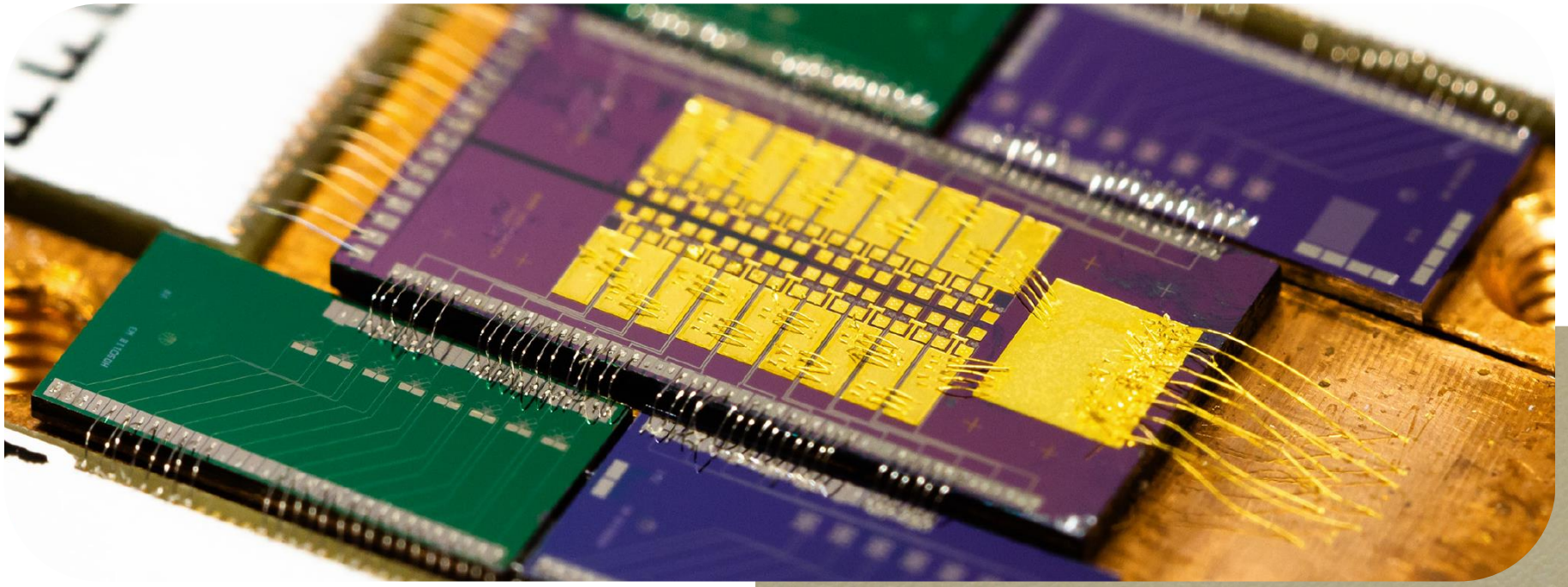

ECHo-1k chip-Au implanted @RISIKO

- High purity ^{163}Ho source
  → activity per pixel $a \approx 1$ Bq
- 4 Front-end chips each with 8 dc-SQUIDs for parallel readout

F. Mantegazzini et al., *JINST* **16** (2021) P08003

ECHo-1k data – Live!

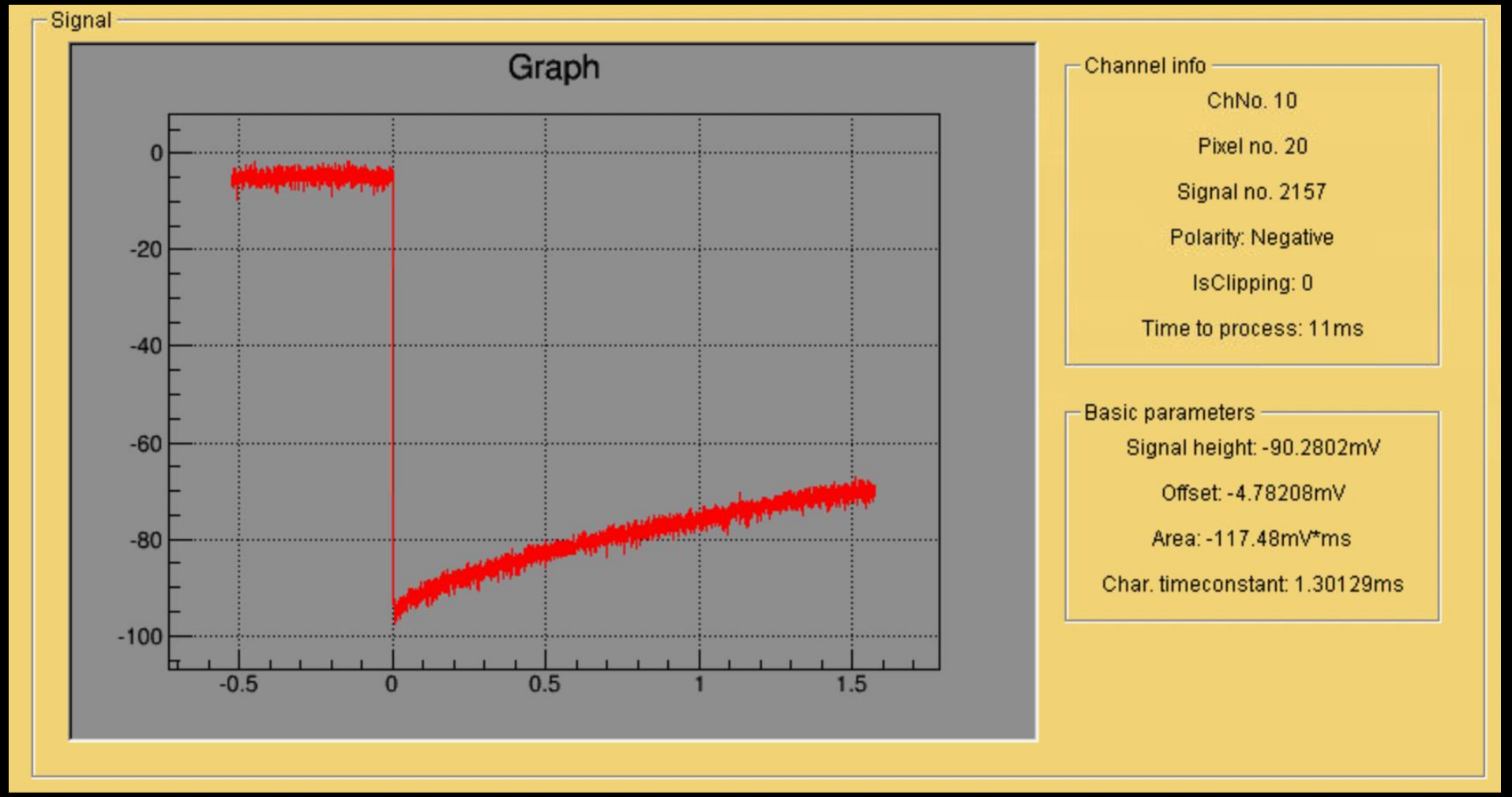

Conclusions

metallic magnetic calorimeters

- are versatile low temperature detectors
- high resolution for all kinds of particles
- wide range of energies
- impressive resolving power

micro-farbrication works

- detector arrays reliably fabricated
- designed performance is reached
- reproducibility of performance

multiplexing

- demonstrated principles

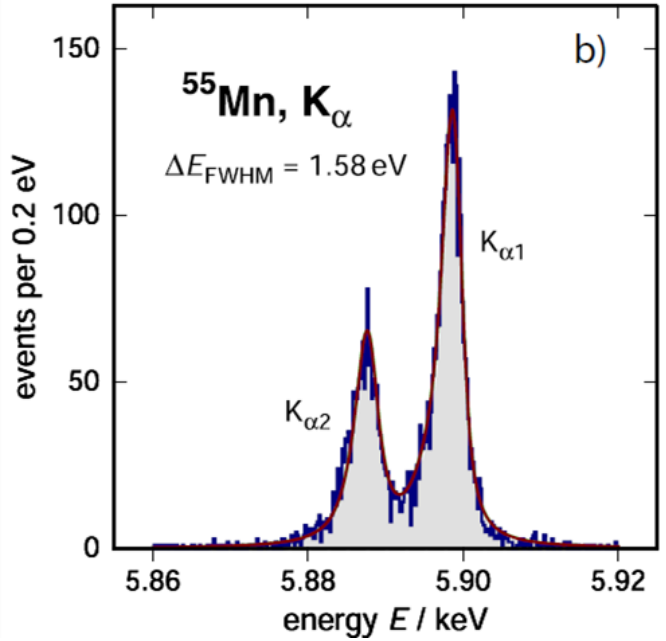

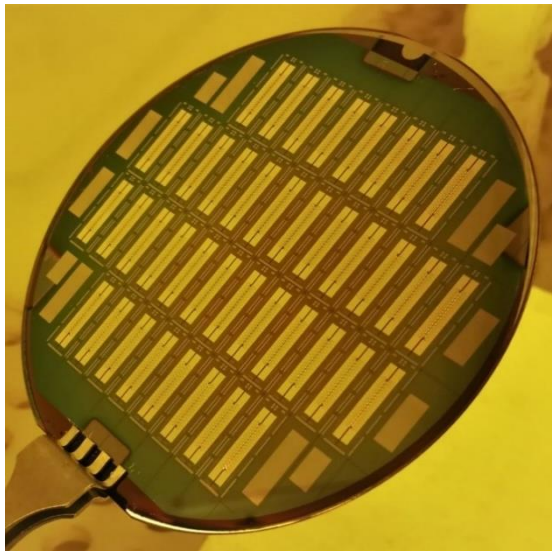

Thank you for the attention!